THE PREDICTION OF SEA-SURFACE TEMPERATURE ANOMALIES USING A 10-LEVEL PRIMITIVE EQUATION MODEL

Kenneth Howard Hunt

NAVAL POSTGRADUATE SCHOOL
Monterey, California

THESIS

THE PREDICTION OF SEA-SURFACE TEMPERATURE ANOMALIES USING A 10-LEVEL PRIMITIVE EQUATION MODEL

by

Kenneth Howard Hunt

September 1975

Thesis Advisor: R. L. Haney

Approved for public release; distribution unlimited.

SECURITY CLASSIFICATION OF THIS PAGE (When Data Entered)

REPORT DOCUMENTATION PAGE		READ INSTRUCTIONS BEFORE COMPLETING FORM
1. REPORT NUMBER	2. GOVT ACCESSION NO.	3. RECIPIENT'S CATALOG NUMBER
4. TITLE (and Subtitle) The Prediction of Sea-Surface Temperature Anomalies Using a 10-Level Primitive Equation Model		5. TYPE OF REPORT & PERIOD COVERED Master's Thesis September 1975 6. PERFORMING ORG. REPORT NUMBER
7. AUTHOR(s) Kenneth Howard Hunt		8. CONTRACT OR GRANT NUMBER(s)
9. PERFORMING ORGANIZATION NAME AND ADDRESS Naval Postgraduate School Monterey, California 93940		10. PROGRAM ELEMENT, PROJECT, TASK AREA & WORK UNIT NUMBERS
11. CONTROLLING OFFICE NAME AND ADDRESS Naval Postgraduate School Monterey, California 93940		12. REPORT DATE September 1975 13. NUMBER OF PAGES 83
14. MONITORING AGENCY NAME & ADDRESS(if different from Controlling Office) Naval Postgraduate School Monterey, California 93940		15. SECURITY CLASS. (of this report) Unclassified 15a. DECLASSIFICATION/DOWNGRADING SCHEDULE

16. DISTRIBUTION STATEMENT (of this Report)

Approved for public release; distribution unlimited.

17. DISTRIBUTION STATEMENT (of the abstract entered in Block 20, if different from Report)

18. SUPPLEMENTARY NOTES

19. KEY WORDS (Continue on reverse side if necessary and identify by block number)

Prediction Sea-Surface
Temperature Anomalies
10-Level Primitive Equation Model

20. ABSTRACT (Continue on reverse side if necessary and identify by block number)

Preliminary experiments in the numerical prediction of large scale sea-surface temperature anomalies are made using a 10-level primitive equation model with 300-km horizontal resolution covering a rectangular basin in the North Pacific. The model is first integrated over an 11-year period to statistical equilibrium using time dependent wind and thermal forcing. The monthly normal climatology, generated by the model in this long term integration, is then used along with observed sea-surface temperature anomalies to

DD FORM 1 JAN 73 1473 EDITION OF 1 NOV 65 IS OBSOLETE
S/N 0102-014-6601 |
(Page 1)

SECURITY CLASSIFICATION OF THIS PAGE (When Data Entered)

define the initial state.

The results show that inclusion of salinity in the model may produce more accurate predictions of high latitude cold anomalies. The most accurate of the predictions removed all of the anomalous diffusion terms in the governing equations. Data for the observed temperature anomalies were not available in depth, thus initialization of the anomalies below the surface was superficial. Consequently, the effects of vertical advection were not fully realized, indicating a need for future experimentation with a more accurately defined initial profile of the anomalies in the initial conditions.

The Prediction of Sea-Surface Temperature Anomalies Using a 10-Level Primitive Equation Model

by

Kenneth Howard Hunt
Lieutenant, United States Navy
B.S., University of Maryland, 1968

Submitted in partial fulfillment of the
requirements for the degree of

MASTER OF SCIENCE IN METEOROLOGY

from the

NAVAL POSTGRADUATE SCHOOL
September 1975

ABSTRACT

Preliminary experiments in the numerical prediction of large scale sea-surface temperature anomalies are made using a 10-level primitive equation model with 300-km horizontal resolution covering a rectangular basin in the North Pacific. The model is first integrated over an 11-year period to statistical equilibrium using time dependent wind and thermal forcing. The monthly normal climatology, generated by the model in this long term integration, is then used along with observed sea-surface temperature anomalies to define the initial state.

The results show that inclusion of salinity in the model may produce more accurate predictions of high latitude cold anomalies. The most accurate of the predictions removed all of the anomalous diffusion terms in the governing equations. Data for the observed temperature anomalies were not available at depth, thus initialization of the anomalies below the surface was superficial. Consequently, the effects of vertical advection were not fully realized, indicating a need for future experimentation with a more accurately defined initial profile of the anomalies in the initial conditions.

TABLE OF CONTENTS

LIST OF FIGURES

ACKNOWLEDGEMENTS

The author wishes to express his appreciation to Dr. Robert L. Haney for his guidance, understanding, and counsel in the preparation of this thesis and to Dr. R. L. Elsberry and Dr. R. T. Williams for reading the thesis and making useful comments.

All predictions were made on the IBM 360 computer at the W. R. Church Computer Center, Naval Postgraduate School, Monterey, California. The author wishes to extend his gratitude to the night-shift personnel at the Computer Center for their assistance and cooperation.

Special appreciation is given to my loving wife whose understanding and patience enabled me to complete the necessary research.

I. INTRODUCTION

For today's meteorologist to make accurate, long range forecasts the understanding of the dynamics of atmospheric behavior is imperative. In the recent meteorological past, the importance of air-sea interactions has been realized and has given the forecaster another potential tool with which to improve his predictions. A better understanding of the interactions between the oceans and the atmosphere will also assist in ocean acoustic forecasting and other Naval operations.

Like the atmosphere, the oceans experience seasonal, monthly, and daily variations in temperature and circulation patterns. Further investigation of these variations reveals the existence of anomalous behavior within the mean temperature and circulation patterns. It is believed that these variations influence directly the atmospheric weather patterns through the exchange of moisture, momentum, and heat across the air-sea interface. This thesis is concerned with the prediction of these anomalous oceanic temperatures and currents.

During the past two decades it has become apparent through the studies of J. Namias and the late J. Bjerknes that the atmospheric response to sea-surface temperature anomalies may be worldwide. Bjerknes (1966, 1969, 1972) has shown that large-scale, sea-surface temperature anomalies exist in the equatorial region and that these anomalies produce a response in the atmosphere which is not limited to that region alone. Likewise, Namias (1959, 1969, 1972b) discusses the possibility that such a response is also present in the middle latitudes. Furthermore, Namias (1969) observed that during several years when intense sea-surface temperature

anomalies were present in the North Pacific Ocean, there were distinct weather patterns over the United States. Because of the above pioneering findings of Namias and Bjerknes, the North Pacific Experiment (NORPAX) was established in which a cooperative scientific effort is being made to understand the causes of these anomalies and their relationship to the atmosphere.

Numerical integrations of coupled ocean-atmosphere models have been reported by Manabe (1969), Bryan (1969), and Wetherald and Manabe (1972). By comparing the results of their coupled model with those of the ocean and atmosphere models integrated separately, these authors showed the significant role ocean circulation plays in determining the state of the atmosphere.

In turning our attention to the oceans, the first attempts at large scale ocean predictions was based upon the use of a prediction equation for the sea-surface temperature (Namias, 1965). In Namias' method, temperature T is a function of x,y,z, and time t. The local rate of change of temperature can be represented by

$$\frac{\partial T}{\partial t} = -u \frac{\partial T}{\partial x} - v \frac{\partial T}{\partial y} - w \frac{\partial T}{\partial z} + q \qquad (1)$$

where q is the rate of change of temperature from non-advective processes. Now if we let $(\bar{})$ denote the long term normal state and $(')$ the anomaly, then the monthly mean can be expressed by

$$T = \bar{T} + T' \ , \ u = \bar{u} + u' \ , \ v = \bar{v} + v' \ , \ w = \bar{w} + w'$$

and

$$q = \bar{q} + q' \ .$$

Then Eq. (1) takes the form:

$$\frac{\partial}{\partial t}(\bar{T} + T') = -(\bar{u}+u') \frac{\partial (\bar{T}+T')}{\partial x} - (\bar{v}+v') \frac{\partial (\bar{T}+T')}{\partial y}$$

$$-(\bar{w}+w') \frac{\partial (\bar{T}+T')}{\partial z} + \bar{q} + q' \ . \qquad (2)$$

Assuming the long term normal temperature satisfies the equation

$$\frac{\partial \bar{T}}{\partial t} = - \bar{u} \frac{\partial \bar{T}}{\partial x} - \bar{v} \frac{\partial \bar{T}}{\partial y} - \bar{w} \frac{\partial \bar{T}}{\partial z} + \bar{q} \qquad (3)$$

subtracting (3) from (2) gives the equation for the temperature anomaly:

$$\frac{\partial T'}{\partial t} = -[(\bar{u}+u') \frac{\partial T'}{\partial x} + (\bar{v}+v') \frac{\partial T'}{\partial y} + (\bar{w}+w') \frac{\partial T'}{\partial z}]$$

$$-[u' \frac{\partial \bar{T}}{\partial x} + v' \frac{\partial \bar{T}}{\partial y} + w' \frac{\partial \bar{T}}{\partial z}] + q' \ . \qquad (4)$$

Namias' first predictions (1965) retained only the advection of the normal temperature by the anomalous currents, $(u' \frac{\partial \bar{T}}{\partial x} + v' \frac{\partial \bar{T}}{\partial y})$, in Eq. (4). The anomalous currents (u', v') were obtained from the anomalous atmospheric wind stress observed during the period of the "forecast" and the long-term normal temperatures ($\bar{T}$) from observations collected by the U. S. Weather Bureau. Since this prediction used data actually observed during the forecast period, it is not a prediction in the true sense and is referred to as a "semiprediction". Although this simple method produced results which correlated positively with the observed temperature changes, Arthur (1966) demonstrated that additional terms should be included in the prediction equation. As a result, Jacob (1967) performed a semiprediction neglecting only the vertical advection terms and the anomalous heating. A quantitative comparison of his results indicated an improvement in the prediction.

More recently, Namias (1972a) has shown that the sea-surface temperature patterns in the North Pacific can be predicted with some success using normal surface currents to advect the anomalies (neglecting all but $-\bar{u}\frac{\partial T'}{\partial x}$, $-\bar{v}\frac{\partial T'}{\partial y}$ on the right side of Eq. (4)). The results of his study (Figs. 1, 2, 3, and 4), which will be discussed in detail later, show the importance of horizontal advection. These results plus the lack of temperature data at depth clearly indicates the need for a completely dynamical model. Therefore, it is the objective of this thesis to predict the evolution of the anomalous temperatures using a numerical model which contains all the advection terms in (4) and a parameterization of mixed layer dynamics as well.

To make a comparative analysis, the period covered by this prediction will be the same as that used by Namias (1972a). Sea-surface temperature anomaly data were also obtained from Namias' 20-year normal observations. It should be noted, however, that this normal data is from the years 1947 to 1966 and is not necessarily representative of the prediction period. Furthermore, due to the aforementioned lack of data at depth, we assume an anomalous temperature profile which decreases linearly from its value at the surface to zero at 150 meters. NORPAX scientists have shown that anomalies exist at depths greater than 150 meters; however, this depth was chosen to correspond more closely to Namias' study which assumed the temperature anomaly to be confined strictly to the surface. Further studies could be conducted varying the vertical profile of the temperature anomaly to determine the importance of the initial condition. The initial anomalous current is geostrophic and its vertical average is zero. Unlike Namias' method which employed the use of observed

climatological data during the entire forecast period, this method uses model-generated climatology only to define the initial conditions. Consequently, following initialization the anomalous and mean fields are completely free to dynamically interact.

II. THE NUMERICAL MODEL

A. BACKGROUND

The basic model used in the following predictions is that of Haney (1974) as modified by Davies (1975). "The model is based upon the hydrostatic and Boussinesq approximations. This means that the ocean is assumed incompressible, and the density is replaced by a constant everywhere except in the hydrostatic equation where it is multiplied by the acceleration of gravity. A major simplification is the neglect of salinity and the assumption that the density is a linear function of temperature alone."[1]

The equations which govern Haney's model are given by

$$\frac{du}{dt} = \frac{-1}{\rho_o a \cos\phi} \frac{\partial p}{\partial \lambda} + fv + \frac{u}{a\cos\phi} v \sin\phi + A_m \nabla^2 u + \kappa \frac{\partial^2 u}{\partial z^2} , \tag{5}$$

$$\frac{dv}{dt} = \frac{-1}{\rho_o a} \frac{\partial p}{\partial \phi} - fu - \frac{u}{a\cos\phi} u \sin\phi + A_m \nabla^2 v + \kappa \frac{\partial^2 v}{\partial z^2} , \tag{6}$$

$$\frac{\partial p}{\partial z} = -\rho g , \tag{7}$$

$$\frac{\partial w}{\partial z} + \frac{1}{a\cos\phi} \left[\frac{\partial u}{\partial \lambda} + \frac{\partial}{\partial \phi} (v \cos\phi)\right] = 0 , \tag{8}$$

$$\frac{dT}{dt} = A_H \nabla^2 T + \kappa \frac{\partial^2 T}{\partial z^2} + \delta_c(T) , \tag{9}$$

$$\rho = \rho_o \left[1 - \alpha(T - T_o)\right] , \tag{10}$$

where the representation of the symbols is as follows:

t time
λ longitude
ϕ latitude

---

[1] Haney, R. L., "A Numerical Study of the Response of an Idealized Ocean to Large Scale Heat and Momentum Flux," J. of Physical Oceanog., V. 4, No. 2, p. 147, 1974.

z height
Ω angular speed of the earth's rotation
f coriolis parameter
a radius of the earth
g acceleration of gravity
u eastward velocity component
v northward velocity component
w vertical velocity component
T temperature
T_o constant reference temperature
ρ density
ρ_o density of water at reference temperature
α coefficient of thermal expansion

B. BOUNDARY CONDITIONS

After Haney (1971) and Davies (1975), the determination of the upper boundary condition in the thermal energy equation is computed by calculating separately the incoming solar radiation (Q_I), the net upward longwave radiation (Q_B), the latent heat exchange (Q_E), and the sensible heat exchange (Q_H). Together, these fluxes define the net downward heat flux as represented by

$$Q = Q_I - (Q_B + Q_E + Q_H) \quad . \tag{11}$$

The back radiation Q_B is calculated from

$$Q_B\ (T_o) = .985(.39 - .05e_a^{1/2})(1 - .6C^2)\ \sigma\ T_o^4 \tag{12}$$

where T_o is the sea surface temperature, e_a the atmospheric vapor pressure at 10 meters, C the fraction of cloud cover, and σ the Stefan-Boltzmann constant. The exchange of latent heat and sensible heat across the ocean-atmosphere interface were computed from

$$Q_E = .622\ \rho_a\ C_D\ |V|\ L\ [e_s(T_o) - e_a]/P_a \tag{13}$$

and

$$Q_H = \rho_a C_D |V| C_p (T_o - T_a) ,$$

respectively, where ρ_a was the density of the air, C_D the drag coefficient, $|V|$ the wind speed at anemometer level, L the latent heat of vaporization, P_a the atmospheric pressure, $e_s(T_o)$ the saturation vapor pressure at the sea-surface temperature, C_p the specific heat of air at constant pressure, and T_a the atmospheric temperature at 10 meters. Incoming solar radiation (Q_I) was calculated with

$$Q_I = S_o(.74 - .6C) \qquad (15)$$

where S_o was the solar insolation incident on a horizontal surface at the top of the atmosphere.

The quantities S_o , C , e_a , T_a and $|V|$ are prescribed functions of latitude (v depends on longitude--see below) and time taken from atmospheric climatological data. The fluxes Q_B , Q_E , and Q_H are additionally dependent on the computed sea-surface temperature, T_o . Therefore, an anomalous sea-surface temperature produces a corresponding anomalous heat flux which has the tendency to remove the temperature anomaly by virtue of the opposing sign in Eq. (11).

"In addition to the thermal forcing, the ocean circulation was also forced by surface winds given on a time-dependent basis. Assuming an average geostrophic inflow angle of 10° and a frictional reduction of velocity by 10%, one could derive the surface stress from the surface geostrophic winds. If u and v are the eastward and northward surface winds, respectively, after inflow and frictional influences are considered, then

$$|V| = (u^2 + v^2)^{1/2}$$

and the wind stress components are

$$\tau_x = \rho_a C_D |V| u$$
$$\tau_y = \rho_a C_D |V| v \text{ ."}^2$$

Therefore, the wind stresses are completely specified since $u(y,t)$ and $v(x,t)$ are completely independent of the ocean temperatures and currents in this experiment. Since the quantities which define the atmospheric forcing are derived from climatological data, this thesis does not concern itself with the response of the ocean to anomalous atmospheric forcing.

Lastly, the ocean bottom is assumed to be flat which requires the vertical velocity to vanish there. Thus integrating the continuity equation up to the surface and applying a free surface boundary condition, one could obtain a prediction for the height of the surface. However, the present method assumes that the ocean surface is not a free surface but rather a balanced surface at which $w = 0$. Therefore, since $w = 0$ at the top and bottom, the vertical average of (8) shows that the vertical average current is non-divergent and consequently can be described by a streamfunction. The streamfunction is predicted from the vorticity equation which is derived from the vertical average of the equations of motion.

C. RESOLUTION AND DATA

To improve the resolution, the 6-level model employed by Haney (1974) was expanded to include 10 levels (Davies, 1975). The vertically expanded

---

[2]Davies, R. W., A Numerical Parameterization of Wind Mixing in a Time-Dependent Baroclinic Oceanic General Circulation Model, M. S. Thesis, Naval Postgraduate School, Monterey, California, 1975, pp 56.

model now has fixed levels at 10, 30, 60, 100, 150, 225, 350, 700, 1500, and 3000 meters.

As mentioned previously, to compare the results with those of Namias (1972a), sea-surface temperature anomaly data covering the same period were obtained from J. Namias of Scripps Institution of Oceanography. The surface temperature data thus obtained covered only the area 20°N to 60°N, 130°E to 110°W in the North Pacific and the grid spacing intervals for the latitude and longitude were 5° and 5° respectively. Therefore, Namias' data were expanded to the equator and to 65°N by extrapolating the anomalous data to zero at the most distant boundaries. Additionally, the data over the entire domain were interpolated to fit the 2.0° latitude and the 2.8° longitude grid spacing of the present model.

As a result of the expansion, the predictions outside the original data field should be ignored. Consequently, for the convenience of the reader, an overlay (Fig. 5) with the locations of ocean vessel stations November (N), Papa (P), and Victor (V) as well as the site of the NORPAX "Pole" experiment, has been superimposed on the normal fields and each related prediction. The superficial land mass boundaries of the NORPAX grid are represented by the shaded area and the original data field by the area between the dashed lines.

D. INITIAL CONDITIONS

To completely define the initial state of the ocean for dynamical predictions, a considerable amount of model climatology was used along with the available observed data. The model climatology was generated by integrating the model over an 11-year period starting from a stratified initial state and using atmospheric data which contained the observed

normal seasonal data. This model climatology was used for initialization and verification as described below. To provide continuity in the atmosphere wind and thermal forcing, the annual mean and amplitude and phase of the first two harmonics were calculated from atmospheric climatological data as defined by Davies (1975). The atmospheric data were averaged along each grid latitudinal line, except for v, the northward component of the surface geostrophic wind, which was averaged along each meridian.

The resulting initial normal currents and the 30, 60, 90 day normal currents at level 2 (30 m) are shown in Figs. 6, 8, 10, and 12, where "initial" is defined as October 15th of year 11. As seen in Figs. 6 and 12, there is an almost negligible change in the normal currents during that period. The corresponding initial, 30, 60, and 90 day normal temperature fields are shown in Figs. 7, 9, 11, and 13. Although there is little change in the temperature gradient in the middle latitudes, the southward movement of the main baroclinic zone indicates a cooling trend which was expected during the winter months.

To begin the predictions, the total field must be defined in the initial conditions. Thus, the normal part of the initial conditions is obtained from the model-generated climatology while the anomalous part is obtained from observations. The observed sea-surface temperature anomalies are extrapolated linearly from observed values at the surface to zero at level 5 (150 meters). This rather arbitrary procedure of defining the anomalous temperatures below the surface is done because of the lack of sub-surface temperature data.

The total current (normal plus anomaly) can be represented by

$$\mathbb{V} = \hat{\mathbb{V}} + \overset{*}{\mathbb{V}} \tag{17}$$

where $(\hat{})$ is the vertical average current, $[\frac{1}{H}\int_{-H}^{o}(\,)dz]$, $(\overset{*}{})$ is the vertical shear current, $[(\,)-(\hat{})]$, and H is the total ocean depth. Expanding (17) into its normal and anomalous parts one obtains

$$\mathbb{V} = \overline{\mathbb{V}} + \mathbb{V}' = \bar{\mathbb{V}} + \hat{\mathbb{V}}' + \overline{\overset{*}{\mathbb{V}}} + \overset{*}{\mathbb{V}}' \tag{18}$$

where $\bar{\mathbb{V}}$ and $\overline{\overset{*}{\mathbb{V}}}$ are the normal part of the vertical average current and the normal part of the vertical shear current respectively. The anomalous part of the vertical average current $(\hat{\mathbb{V}}')$ is assumed to be zero and the anomalous part of the vertical shear current $(\overset{*}{\mathbb{V}}')$ is the geostrophic current calculated from the above temperature anomaly using the thermal wind relation. Since

$$\mathbb{V}_g = \frac{1}{\rho_o f}\,\mathbb{k} \times \nabla p \ ,$$

taking the partial derivative with respect to z produces

$$\frac{\partial \mathbb{V}_g}{\partial z} = \frac{1}{\rho_o f}\,\mathbb{k} \times \nabla(-\rho q) \ .$$

Substituting (10) for ρ

$$\rho = -\rho_o\,\alpha\,T + \text{constant} \ ,$$

where the gradient of ρ becomes

$$\nabla\rho = -\rho_o\,\alpha\,g\,\nabla\,T \ .$$

Therefore,

$$\frac{\partial \mathbb{V}_g}{\partial z} = \frac{\alpha g}{f} \mathbb{k} \times \nabla T \qquad \text{(thermal wind relation).}$$

It is now assumed that the anomalous part of the vertical shear current satisfies this relationship,

$$\frac{\partial \overset{*}{\mathbb{V}}'}{\partial z} = \frac{\alpha g}{f} \mathbb{k} \times \nabla T' \ .$$

Then integrating from -H to some depth z

$$\overset{*}{\mathbb{V}}'(z) = \overset{*}{\mathbb{V}}'(-H) + \frac{\alpha g}{f} \mathbb{k} \times \nabla \int_{-H}^{z} T' d\zeta \tag{19}$$

where $\overset{*}{\mathbb{V}}'(-h)$ is unknown. If the vertical average of $\overset{*}{\mathbb{V}}'$ is taken, then this quantity can be set equal to zero by definition. Thus, from (19)

$$\hat{\overset{*}{\mathbb{V}}}' = \frac{1}{H} \int_{-H}^{0} \overset{*}{\mathbb{V}}'(-H) dz + \frac{\alpha g}{f} \mathbb{k} \times \nabla \frac{1}{H} \int_{-H}^{0} \left(\int_{-H}^{z} T' d\zeta \right) dz \equiv 0 \ ,$$

or

$$\overset{*}{\mathbb{V}}'(-H) + \frac{\alpha g}{f} \mathbb{k} \times \nabla \frac{1}{H} \int_{-H}^{0} \left(\int_{-H}^{z} T' d\zeta \right) dz \equiv 0 \ . \tag{20}$$

Then (20) can be solved for $\overset{*}{\mathbb{V}}'(-H)$ and substituting into (19) to give the result

$$\overset{*}{\mathbb{V}}'(z) = \frac{\alpha g}{f} \mathbb{k} \times \nabla \Big[\underbrace{\int_{-H}^{z} T' dz}_{a} - \underbrace{\frac{1}{H} \int_{-H}^{0} \left(\int_{-H}^{z} T' d\zeta \right) dz}_{b} \Big] \ . \tag{21}$$

In Eq. (21) f is not allowed to become smaller than its value at 13.25°N. This geostrophic approximation to the vertical shear current anomaly is then used as the initial condition in the present model.

Having defined the initial temperature and currents by combining the model generated normal fields with the observed anomaly fields, the model is run for 90 days of simulated time. During this time, the total temperatures and currents interact and evolve together. At any given time later (e.g., 60 days) the predicted anomaly is defined to be the total field predicted for that time minus the model generated normal for that same time.

E. THE PREDICTION EQUATION

Since several cases were studied using variations of the thermodynamic prediction Eq. (9) which governs the total temperature field, a detailed analysis of that equation follows.

Neglecting the convective adjustment ($\delta_c(T)$) in the analysis, (9) can be written

$$\frac{dT}{dt} = A \nabla_H^2 T + \kappa \frac{\partial^2 T}{\partial z^2} . \tag{22}$$

Expanding (22)

$$\frac{\partial T}{\partial t} + u \frac{\partial T}{\partial x} + v \frac{\partial T}{\partial y} + w \frac{\partial T}{\partial z} = A\left(\frac{\partial^2 T}{\partial x^2} + \frac{\partial^2 T}{\partial y^2} \right) + \kappa \frac{\partial^2 T}{\partial z^2} \tag{23}$$

and substituting further for the normal and anomalous parts, (23) takes the form

$$\frac{\partial \bar{T}}{\partial t} + \frac{\partial T'}{\partial t} = -[\bar{u}\frac{\partial \bar{T}}{\partial x} + \bar{u}\frac{\partial T'}{\partial x} + u'\frac{\partial \bar{T}}{\partial x} + u'\frac{\partial T'}{\partial x} + \bar{v}\frac{\partial \bar{T}}{\partial y} + \bar{v}\frac{\partial T'}{\partial y}$$

$$+ v'\frac{\partial \bar{T}}{\partial y} + v'\frac{\partial T'}{\partial y} + \bar{w}\frac{\partial \bar{T}}{\partial z} + \bar{w}\frac{\partial T'}{\partial z} + w'\frac{\partial \bar{T}}{\partial z} + w'\frac{\partial T'}{\partial z}]$$

$$+ A[\frac{\partial^2 \bar{T}}{\partial x^2} + \frac{\partial^2 T'}{\partial x^2} + \frac{\partial^2 \bar{T}}{\partial y^2} + \frac{\partial^2 T'}{\partial y^2}] + K[\frac{\partial^2 \bar{T}}{\partial z^2} + \frac{\partial^2 T'}{\partial z^2}] \quad . \tag{24}$$

Setting T', u', v', and w' equal to zero, then the normal field can be represented by

$$\frac{\partial \bar{T}}{\partial z} = -[\bar{u}\frac{\partial \bar{T}}{\partial x} + \bar{v}\frac{\partial \bar{T}}{\partial y} + \bar{w}\frac{\partial \bar{T}}{\partial z}] + A[\frac{\partial^2 \bar{T}}{\partial x^2} + \frac{\partial^2 \bar{T}}{\partial y^2}] + K\frac{\partial^2 \bar{T}}{\partial z^2} \quad . \tag{25}$$

Subtracting (25) from (24), the equation governing the anomalous temperatures becomes,

$$\frac{\partial T'}{\partial t} = -[\bar{u}\frac{\partial T'}{\partial x} + u'\frac{\partial \bar{T}}{\partial x} + u'\frac{\partial T'}{\partial x} + \bar{v}\frac{\partial T'}{\partial y} + v'\frac{\partial \bar{T}}{\partial y} + v'\frac{\partial T'}{\partial y} + \bar{w}\frac{\partial T'}{\partial z}$$

$$+ w'\frac{\partial \bar{T}}{\partial z} + w'\frac{\partial T'}{\partial z}] + A[\frac{\partial^2 T'}{\partial x^2} + \frac{\partial^2 T'}{\partial y^2}] + K\frac{\partial^2 T'}{\partial z^2} \quad . \tag{26}$$

The following investigation will reveal that initially $\mathbb{V}' \cdot \nabla T' = 0$ by analysis of (21). If we let "D" represent the depth at which the temperature anomaly becomes zero as defined earlier, then the temperature anomaly (T') at some level $z < 0$ is

$$\frac{T'(x,y,0) - T(x,y,-D)}{D} = \frac{T'(x,y,0) - T'}{-z}$$

where $T'(x,y,0)$ is the sea-surface temperature anomaly and $T'(x,y,-D)$ is the temperature anomaly at D = 150 meters. Since $T'(x,y,-D) = 0$ by definition, then

$$T' = T'(x,y,0)\left(1 + \frac{z}{D}\right) . \tag{27}$$

Substituting (27) into term (a) of (21) gives

$$\int_{-H}^{z} T'dz = F(z)\ T'(x,y,0), \tag{28}$$

where

$$F(z) = \int_{-H}^{z} \left(1 + \frac{\zeta}{D}\right)d\zeta$$

and (ζ) is a dummy variable representing the vertical coordinate. Likewise, (28) can be substituted into term (b) of (21) to produce

$$\frac{1}{H}\int_{-H}^{0}\left(\int_{-H}^{z} T'd\zeta\right)dz = \frac{1}{H}\int_{-H}^{0} F(z)\ T'(x,y,0)dz$$

$$= \hat{F}\ T'(x,y,0) . \tag{29}$$

Therefore, (21) becomes

$$\overset{*}{W}' = \frac{\alpha g}{f}\ k \times \nabla_H[F(z)\ T'(x,y,0) - \hat{F}\ T'(x,y,0)]$$

or by factoring $T'(x,y,0)$

$$\overset{*}{W}' = \frac{\alpha g}{f}\ k \times \nabla_H[T'(x,y,0)\ (F(z) - \hat{F})] .$$

From this, it is clear that $F(z)$ and $\hat{F}$ are not functions of x and y and can be brought outside the "del" operator allowing

$$\overset{*}{\mathbb{V}}' = \frac{\alpha g}{f} (F(z) - \hat{F}) \mathbb{k} \times \nabla_H T'(x,y,0) \ . \tag{30}$$

Consequently,

$$\overset{*}{\mathbb{V}}' \cdot \nabla_H T' = \frac{\alpha g}{f}(F(z)-\hat{F}) [\mathbb{k} \times \nabla_H T'(x,y,0) \cdot \nabla_H T'(x,y,0) (1 + \frac{z}{D})]$$

$$= \frac{\alpha g}{f}(F(z)-\hat{F}) (1+ \frac{z}{D}) [\underbrace{\mathbb{k} \times \nabla_H T'(x,y,0)}_{a} \cdot \underbrace{\nabla_H T'(x,y,0)}_{b}] \tag{31}$$

and since term (a) of (31) is parallel to the anomalous temperature field and term (b) of (31) is perpendicular to the same field, then $\overset{*}{\mathbb{V}}' \cdot \nabla_H T' = 0$. Since $\hat{\mathbb{V}}' = 0$, we have

$$\mathbb{V}' \cdot \nabla_H T' = 0 \ ,$$

which allows $u' \frac{\partial T'}{\partial x}$ and $v' \frac{\partial T'}{\partial y}$ to be neglected in (26). Figures 14 and 15 clearly show that initially the anomalous currents are geostrophic and parallel to the anomalous isotherms. It should be noted that these currents need not remain parallel to the anomalous isotherms or geostrophic during the prediction period; however, careful examination of the predictions indicates they do. It is not surprising that this type of motion remains geostrophic, but it is surprising that it remains equivalent barotrophic. Therefore, for the purpose of this interpretation, we will assume that $\mathbb{V}' \cdot \nabla_H T'$ is negligible during the forecast period.

Additionally, $w'\frac{\partial T'}{\partial z}$ can be further evaluated. From the continuity equation (8),

$$\frac{\partial w}{\partial z} + \nabla_H \cdot \mathbb{V} = 0 ,$$

then

$$\frac{\partial \bar{w}}{\partial z} + \nabla_H \cdot \bar{\mathbb{V}} + \frac{\partial w'}{\partial z} + \nabla_H \cdot \mathbb{V}' = 0$$

where

$$\frac{\partial \bar{w}}{\partial z} + \nabla_H \cdot \bar{\mathbb{V}} = 0 ,$$

implying

$$\frac{\partial w'}{\partial z} + \nabla_H \cdot \mathbb{V}' = 0 .$$

Thus integrating up from the level z to the surface $z = 0$,

$$w' = \int_z^0 \nabla_H \cdot \mathbb{V}' \, dz + w'(0) \tag{32}$$

where $w'(0) = 0$ as defined by the boundary conditions. Therefore, (32) can be written

$$w' = \int_z^0 \nabla_H \cdot \mathbb{V}' \, dz , \tag{33}$$

and since $\nabla_H \cdot \hat{\mathbb{V}}' = 0$, $\nabla_H \cdot \mathbb{V}' = \nabla_H \cdot \overset{*}{\mathbb{V}}'$ allowing the substitution of (30) into (33) as

$$w' = \alpha g \int_z^0 \nabla_H \cdot \left[\frac{(F(z)-\hat{F})}{f} \mathbb{k} \times \nabla_H T'(x,y,0)\right] dz . \tag{34}$$

Since the coriolis parameter (f) is a function of y, and T'(x,y,0) is not a function of z, Eq. (34) becomes

$$w' = \nabla_H \cdot \left[\frac{\alpha g}{f} [k \times \nabla_H T'(x,y,0)\ \tilde{F}(z)]\right] \tag{35}$$

where

$$\tilde{F}(z) = \int_z^0 (F(z) - \hat{F})\ dz\ .$$

Hence, evaluating (35)

$$w' = \left[\nabla_H \cdot \left(-\frac{\alpha g}{f} \frac{\partial T'(x,y,0)}{\partial y}\ \tilde{i} + \frac{\alpha g}{f} \frac{\partial T'(x,y,0)}{\partial x}\ \tilde{j}\right)\ \tilde{F}(z)\right]\ . \tag{36}$$

If we denote the geostrophic current, integrated from the level z to the surface z = 0 by (Ug, Vg) ,

$$Ug(z) = -\frac{\alpha g}{f} \frac{\partial T'(x,y,0)}{\partial y}\ \tilde{F}(z)$$

and

$$Vg(z) = \frac{\alpha g}{f} \frac{\partial T'(x,y,0)}{\partial x}\ \tilde{F}(z)\ ,$$

then (36) can be written

$$w' = \left[\frac{\partial}{\partial x}\ (Ug) + \frac{\partial}{\partial y}\ (Vg)\right]\ . \tag{37}$$

Therefore,

$$w' = -\frac{\alpha g}{f^2}\ \frac{\partial f}{\partial y}\ \frac{\partial T'(x,y,0)}{\partial x}\ \tilde{F}(z) = -\frac{\beta}{f}\ Vg(z)$$

and so,

$$w'\ \frac{\partial T'}{\partial z} = -\frac{\beta}{f}\ Vg(z)\ \frac{\partial T'}{\partial z}\ . \tag{38}$$

The approximation for the vertical velocity w' applies after integration begins as well as initially. This result shows that w' is the vertical motion produced by the divergence of the goestrophic current. Thus, a northward moving layer of surface water (Vg > 0) converges to produce sinking motion below the surface (w' < 0), while southward moving surface water (Vg < 0) diverges and produces rising motion below the surface (w' > 0). As a result of the above evaluated terms of (26), the final prediction equation for the anomalous temperatures becomes

$$\begin{matrix} & 1 & & 2 & & 3 & & 4 & & 5 & & 6 \end{matrix}$$

$$\frac{\partial T'}{\partial t} = -[\bar{u}\frac{\partial T'}{\partial x} + \bar{v}\frac{\partial T'}{\partial y} + u'\frac{\partial \bar{T}}{\partial x} + v'\frac{\partial \bar{T}}{\partial y} + \bar{w}\frac{\partial T'}{\partial z} - \frac{\beta}{f}Vg(z)\frac{\partial \bar{T}}{\partial z}$$

$$- \frac{\beta}{f}Vg(z)\frac{\partial T'}{\partial z}] + A[\frac{\partial^2 T'}{\partial x^2} + \frac{\partial^2 T'}{\partial y^2}] + \kappa\frac{\partial^2 T'}{\partial z^2} \quad . \qquad (39)$$

$$\begin{matrix} & 7 & & & & 8 & & & & 9 & & \end{matrix}$$

The first two terms on the right-hand side of Eq. (39) represent the horizontal advection of the anomalous temperature by the normal current. These are the only terms used by Namias (1972a) to make his prediction. Terms 3 and 4 are the horizontal advection of the normal temperature by the anomalous current. Term 5 is the vertical advection of the anomalous temperature by the normal current. The vertical advection of the normal temperature by the anomalous current and the vertical advection of the anomalous temperature by the anomalous current are terms 6 and 7 respectively. Term 8 is the horizontal eddy diffusion of the anomalous temperature and term 9 is the vertical eddy diffusion of the anomalous temperature which also includes the anomalous part of the surface heat flux (see discussion below (15)).

The motivation behind the inclusion of all the terms of (39) is, of course, to make a more accurate prediction. As a result of Jacob's (1967) work, which showed an improvement over Namias' predictions (1972a) by including terms 3 and 4 of (39), and since vertical advection is so important in the theory of the permanent thermocline, the implication is that all the advection terms should be included when making a prediction of the sea-surface temperature anomaly.

III. RESULTS

Before discussing the results of the predictions generated by the complete dynamical model, a brief description of the observed anomalous temperature fields and the results of Namias'(1972a) predictions follows. The initial, 30, 60, and 90 day observed anomalous temperature fields, as seen in Figs. 15, 16, 17 and 18, are averages over three months centered about the months of October, November, December, and January respectively. That is, the initial anomalous temperature field is the average of the anomalous temperatures for the months September, October, and November (i.e., the Fall season) of 1971.

From Figs. 15 through 18 two cold anomalies and one warm anomaly appear to dominate the area of interest. The cold anomaly near the western boundary is observed to decrease in amplitude almost linearly during the first 60 days with a small southward movement. The double cell cold anomaly near the northeast boundary decreases in amplitude in the western part but maintains its relative amplitude and position in the eastern part. Finally, the warm anomaly near the center of Fig. 15, increases in amplitude with the leading edge of the maximum anomalous temperature contour moving eastward some 13° longitude.

If one observes Namias' 90 day prediction of the warm anomaly (Fig. 4), as described above, the easterly movement of the anomaly, as advected by the normal winter sea-surface currents (Fig. 3), is a good approximation. However, the amplitude of the anomaly in his prediction remains relatively constant, when it was observed to increase. In an

attempt to explain this discrepancy, Namias calculated the surface heat fluxes, but the results obtained indicated a negligible (and at times opposed) role of these fluxes. It is therefore suggested that the over-simplified use of the prediction equation, as described earlier, and the lack of data at depth is responsible for not predicting accurately the amplitude of the anomaly.

Attempting to improve the predictions made by Namias (1972a), the completely dynamical model of this thesis was run for a corresponding 90-day period using the initial anomalous temperature field (Fig. 15) and the model generated climatological data along with the boundary conditions as described earlier. Four cases using variations in the boundary conditions and this prediction equation are discussed below.

A brief description of the four cases will be given first, followed by a qualitative discussion of the results obtained.

CASE 1:

In CASE 1 the anomalous temperature prediction contained all the terms implied by Eq. (39). The results of CASE 1 are shown in Figs. 19-24.

CASE 2:

In CASE 2 the model calculated the 90 day prediction as in CASE 1 except in the surface thermal boundary condition, Eqs. (12), (13), and (14), the normal climatological sea-surface temperatures were substituted for the predicted sea-surface temperatures. This effectively removed the anomalous part of the surface heat flux. The results of CASE 2 are shown in Figs. 25-30.

CASE 3:

CASE 3 is similar to CASE 2 except normal climatological temperatures were substituted in place of the predicted temperatures in the diffusion terms of (9). This effectively eliminates the anomalous diffusion terms, $[A(\frac{\partial^2 T'}{\partial x^2} + \frac{\partial^2 T'}{\partial y^2}), \kappa \frac{\partial^2 T'}{\partial z^2}]$, from (39). The results of CASE 3 are shown in Figs. 31-36.

CASE 4:

CASE 4 is similar to CASE 3 except normal climatological currents $(\bar{u},\bar{v})$ were substituted for the predicted currents in the diffusion terms ($A \nabla^2 u$, $\kappa \frac{\partial^2 u}{\partial z^2}$ and $A \nabla^2 v$, $\kappa \frac{\partial^2 v}{\partial z^2}$) of the primitive Eqs. (5) and (6). This has the effect of removing the anomalous diffusion terms ($A \nabla^2 u'$, $\kappa \frac{\partial^2 u'}{\partial z^2}$ and $A \nabla^2 v'$, $\kappa \frac{\partial^2 v'}{\partial z^2}$) from the equations governing the anomalous currents. The results of CASE 4 are shown in Figs. 37-42.

Concentrating on the results of the anomalous temperature predictions of CASE 1 (Figs. 15, 20, 22, and 24), one observes that all the anomalies appear to decrease in amplitude with the cold anomalies disappearing completely by the end of that 90 day prediction. The amplitude of the warm anomaly initially was found to be .6°C located at 168°W, 40°N and is reduced to .1°C after 90 days with its center at 162°W, 37°N. As a result of the above observations, cases 2, 3, and 4 were designed to determine the cause of the amplitude decrease or disappearance of these anomalies. Furthermore, the western edge of the warm anomaly is observed to move eastward while the eastern edge remains relatively stationary. Below 20°N some anomalous activity appears to have been generated; however, since this lies outside the area of initial observed data, it is disregarded and further discussion of this region will be omitted.

As in CASE 1, the cold anomaly at the northeast boundary disappears in CASE 2 (Figs. 15, 26, 28, and 30). Analyzing the initial vertical profile of the total temperature field, it was found that the lapse rate was unstable thereby implying that convective adjustment (term $\delta_c(T)$ in (9)), is the cause of the cold anomaly vanishing. This rapid disappearance of the cold anomaly immediately raises the question of the importance of salinity. If salinity were included in the present model, it is speculated that the cold anomaly could maintain itself. That is, the cold anomaly at the surface would not necessarily be unstable if a (negative) salinity anomaly were present to stabilize the water in the column. Another possibility is that salinity is negligible, but the cold anomaly extends all the way to the ocean floor. However, this explanation seems less likely since it indicates the presence of such a large anomaly of heat content.

Investigation of the initial vertical temperature profile of the total field in the vicinity of the cold anomaly near the western boundary reveals that it too is convectively unstable. However, this anomaly damps less rapidly in CASE 2 than does the cold anomaly at the northeast boundary which would indicate its decrease in amplitude is not entirely due to convective adjustment. Additionally, the amplitude of the central warm anomaly was found to decrease less (to a value of .2°C) than in CASE 1. Except for the above two differences, the 60 and 90 day predictions of cases 1 and 2 are relatively similar. Therefore, with respect to the observations of the first two cases, it is concluded that the anomalous surface heat flux induced by the anomaly itself is not the major cause of the damping of the anomalies, and that convective adjustment is the major cause of the cold anomalies vanishing. The effects of diffusion will be discussed in cases 3 and 4 below.

Figures 15, 32, 34, and 36 show the results of CASE 3, in which there is no eddy diffusion of the temperature anomaly. It is seen that the cold anomaly at the northeast boundary still disappears as in cases 1 and 2. The western cold anomaly, however, appears to maintain its magnitude for a greater duration than in the previous two cases; the greatest difference occurring during the 60 to 90 day prediction period. The western edge of the warm anomaly moves eastward about the same distance as before but its shape is altered and the eastern edge remains unchanged as in cases 1 and 2. The major difference observed in CASE 3 is that the maximum amplitude center of the warm anomaly only decreases from .6°C initially to .4°C at the end of the 90 day prediction. Consequently, the results of CASE 3 imply that the anomalous diffusion terms of (39) were significant in producing the heavy damping in cases 1 and 2. Since removing the anomalous diffusion terms of (39) improved the results of the prediction considerably, but did not completely eliminate all of the damping, CASE 4 was devised in which the diffusion of the anomalous currents was also removed. The removal of these additional diffusion terms should eliminate some damping because of the dependence of the temperature on the currents through the geostrophic relationship as discussed previously.

With respect to dissipation, movement, and amplitude of the anomalies, CASE 4 (Figs. 15, 38, 40, and 42) produced results nearly identical to those of CASE 3. Therefore, it is concluded that the diffusion terms governing anomalous currents in the primitive equations are seemingly unimportant in the prediction of sea-surface temperature anomalies. Nevertheless, CASE 4 represents a more consistent model in that there is no diffusion of either the anomalous currents or temperature.

If one now compares the results of Namias' prediction (Fig. 4) with the results found in this study using a completely dynamical model, it is first observed that the 0° isotherm of the warm anomaly has about the same configuration and location. Secondly, the location of the center of maximum amplitude in the predicted warm anomaly is much closer to the observed 90 day position in Namias' study than in this study. However, if one closely examines the location of this anomaly center in Figs. 15 and 16, it is seen that the anomaly center moves eastward almost 15° of longitude during the first 30 days and then remains relatively stationary. This observation would imply that the movement of the anomaly's center is not due simply to advection alone as indicated in Namias' prediction. Lastly, the amplitude of the predicted warm anomaly decreases in all cases of this study but the amplitude of the same anomaly in Namias' prediction remains constant as expected when employing horizontal advection alone. Therefore, the vertical advection in this model plays an important role in the evolution of such an anomaly. Whether that role in the present prediction or any future predictions is simulated accurately by the model depends critically on the vertical profile assumed for the anomaly.

IV. CONCLUSIONS

This study has shown that the method of prediction using model generated climatology along with observed temperature anomalies in a fully dynamical numerical model of the ocean circulation can be successful. Also, the simple geostrophic initial conditions for the anomalous currents is successful away from the equator. However, the quality of the above results depends on the precise initial data available.

In view of this study, the need for temperature data (normal and anomalous)in the mixed layers of the ocean is concluded to be the dominating factor influencing the prediction of the sea-surface temperature anomalies. This appears quite evident from our observation discussed above in reference to Figs. 15 and 16. Since this rapid movement of the anomaly center cannot be explained by horizontal advection alone, it is speculated that a sub-surface warm anomaly may have existed downstream which was brought to the surface. Thus, vertical advection may have played a significant role; however, the lack of data beneath the surface makes these speculations virtually impossible to investigate.

The present model, with no salinity, cannot accurately predict the evolution of high latitude cold anomalies which do not extend to the ocean floor. Therefore, initialization should include salinity; however, at present, large scale anomalous salinity data is not available.

When comparing the results of cases 3 and 4, it is observed that the removal of the diffusion terms governing the anomalous currents had little effect, if any, on the 90 day prediction. Thus, further

predictions using a dynamical model should, for consistency, omit all of the anomalous diffusion terms (CASE 4).

Although the results of this study did not produce predictions which corresponded exactly with the observed anomaly field, the use of a fully dynamical model in making these predictions has given us a greater insight as to the role played by vertical advection and diffusion. It is therefore believed that further studies should be conducted using this fully dynamical model with more accurate initial data and with salinity included.

Additionally, this study uses only climatological data to define the atmospheric forcing. However, an anomalous atmosphere would produce anomalous heating and wind stresses which could produce anomalous features in the ocean. For example, Namias (1965) investigated the effects of an anomalous wind stress and showed that this anomalous atmospheric forcing may be important in some cases. Thus, further investigations should be conducted to determine the response of the ocean to various anomalous atmospheric forcing.

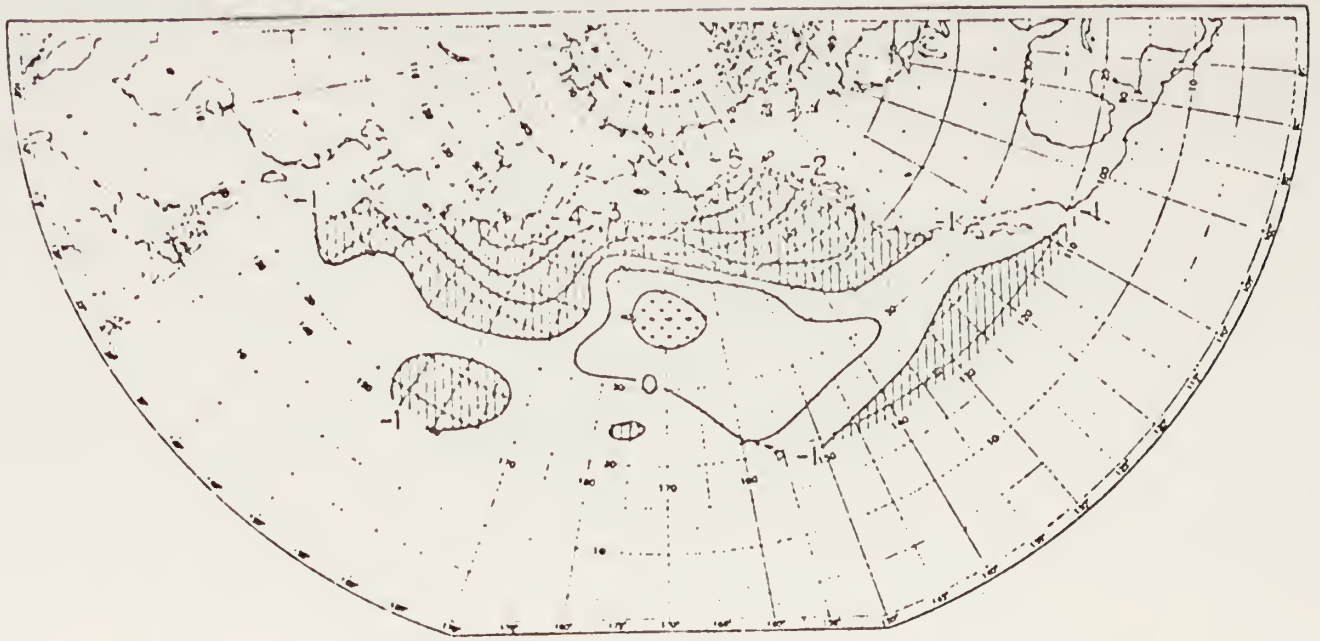

Figure 1. Fall 1971 sea-surface temperature departure(°F) from the 20-year mean 1947-1966. Areas less than -1F are hatched; areas greater than +1F are stippled. From Namias(1972a,fig.2).

Figure 2. Winter 1971-72 sea-surface temperature departure(°F) from the 20-year mean 1947-66. Shading as in Fig.1. From Namias(1972a,fig.3).

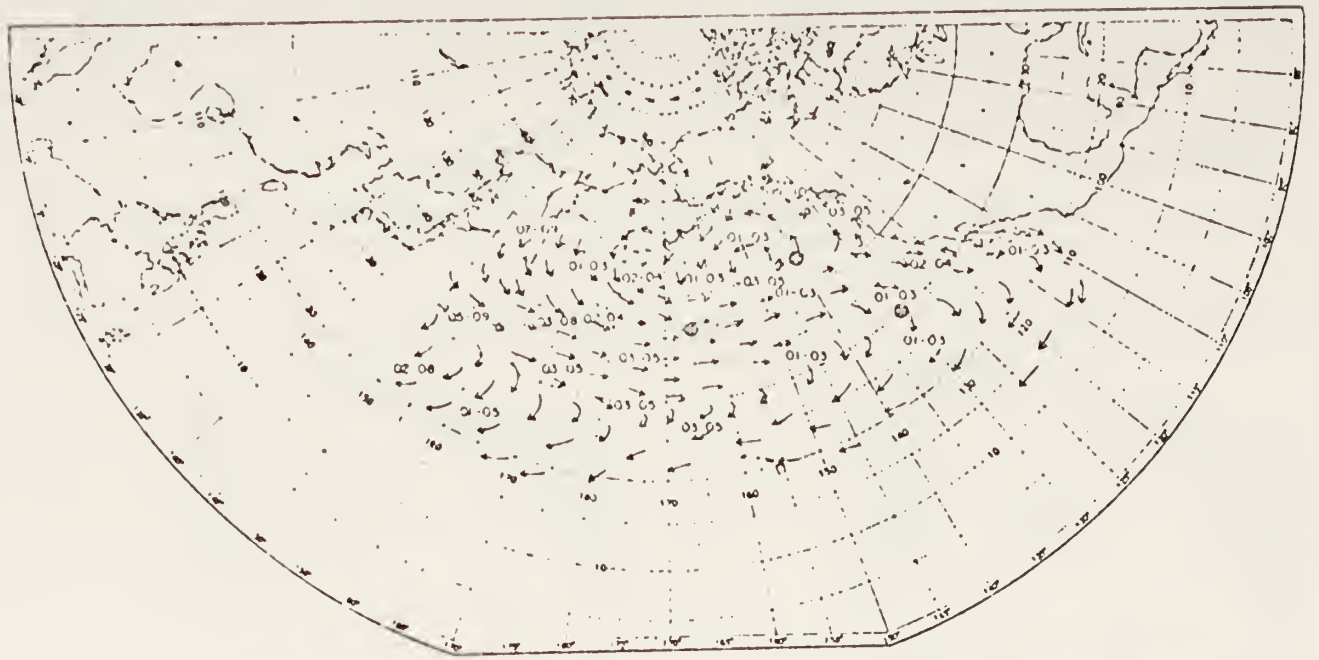

Figure 3. North Pacific winter surface currents(abbreviated from chart shown in Department of Commerce atlas,1961). From Namias(1972a,fig.8).

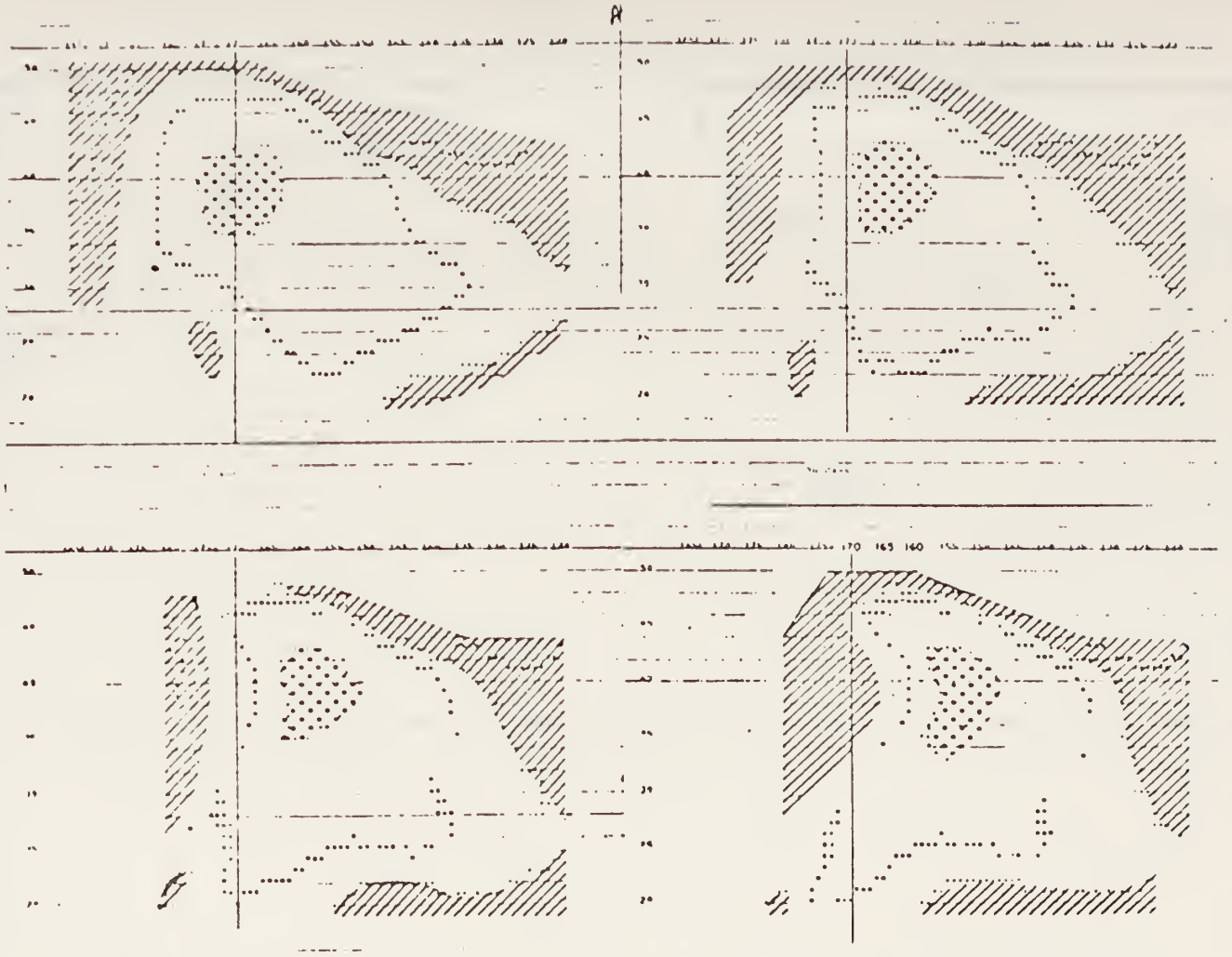

Figure 4. Initial (a) and predicted (b,c,and d) sea-surface temperature anomalies after 30,60, and 90 days. Hatched areas show anomalies ranging between -1F and -2F; stippled areas indicate anomalies >1F. Heavy vertical line marks 170W. From Namias(1972a,fig.9).

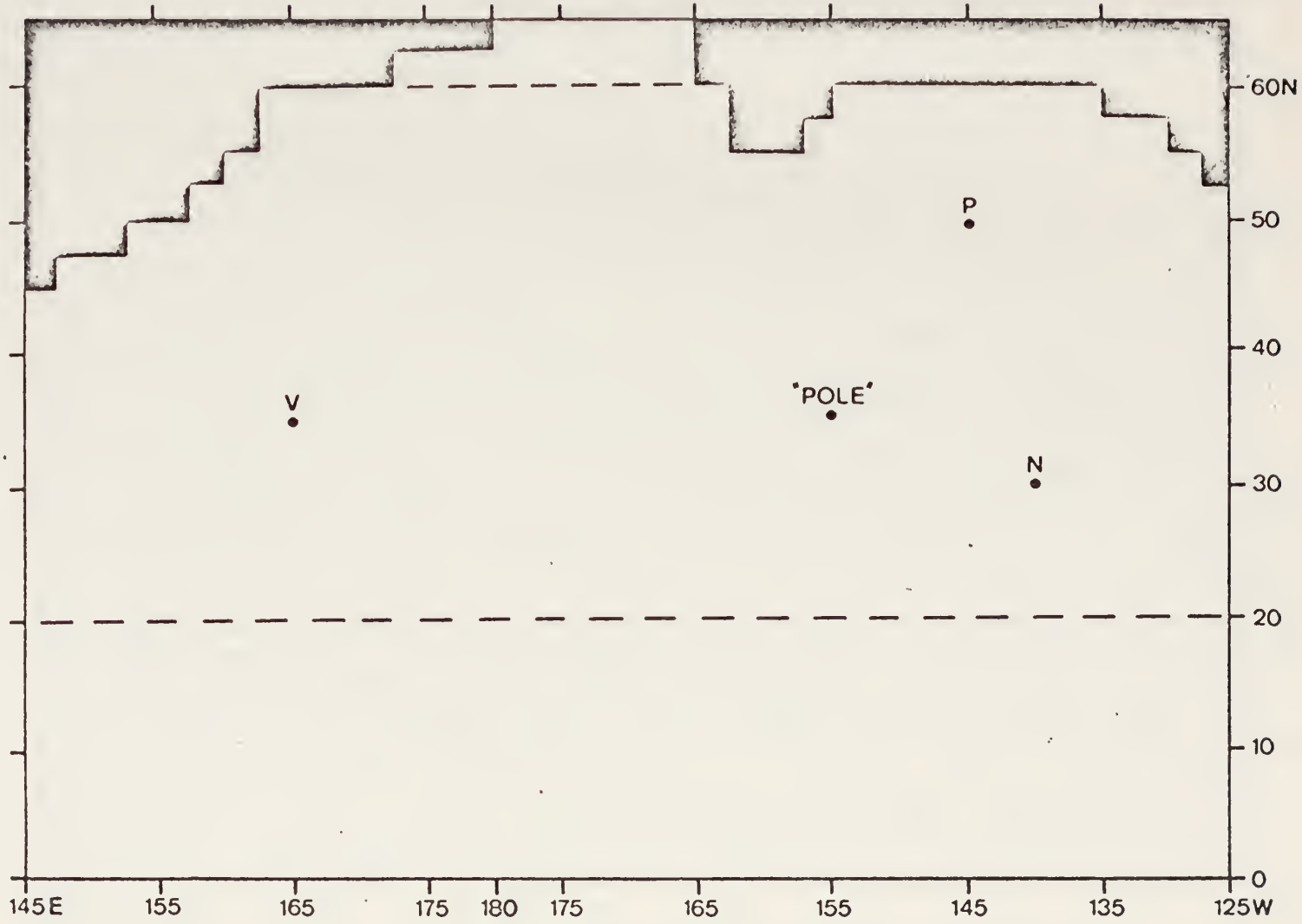

Figure 5. Domain of predictions.

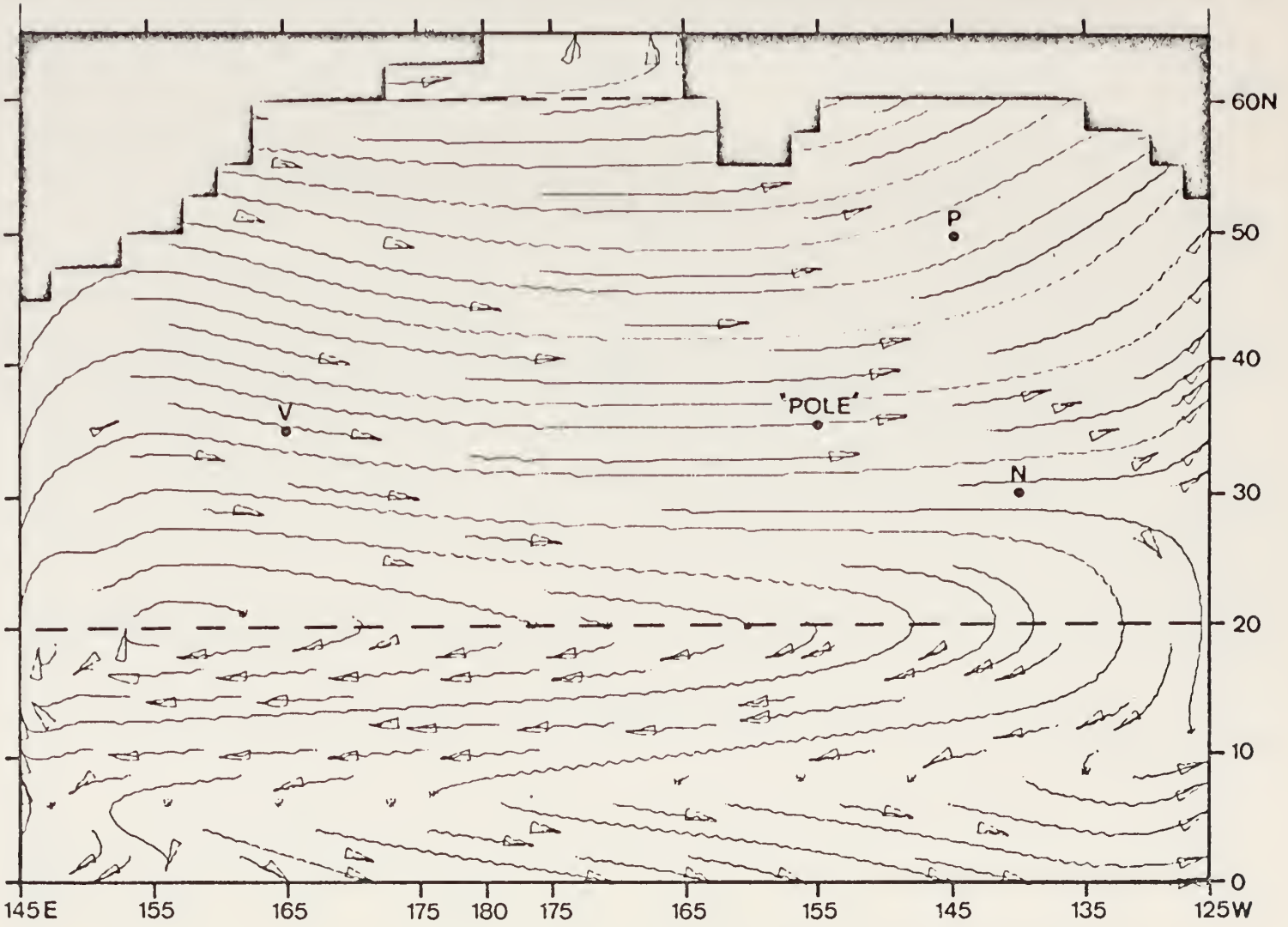

Figure 6. Initial normal currents generated by 11-year integration of model.

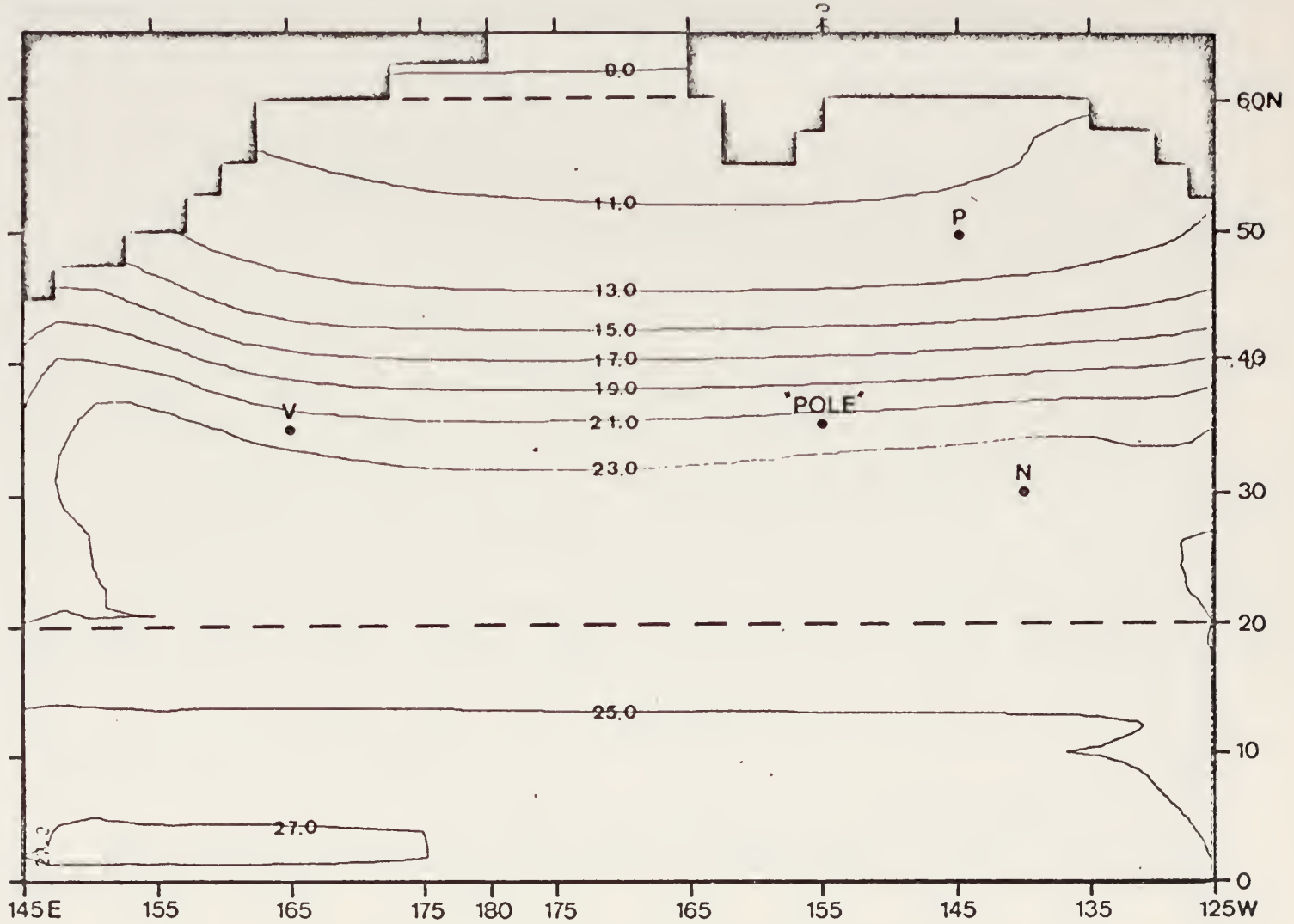

Figure 7. Initial normal temperatures generated by 11-year integration of model.

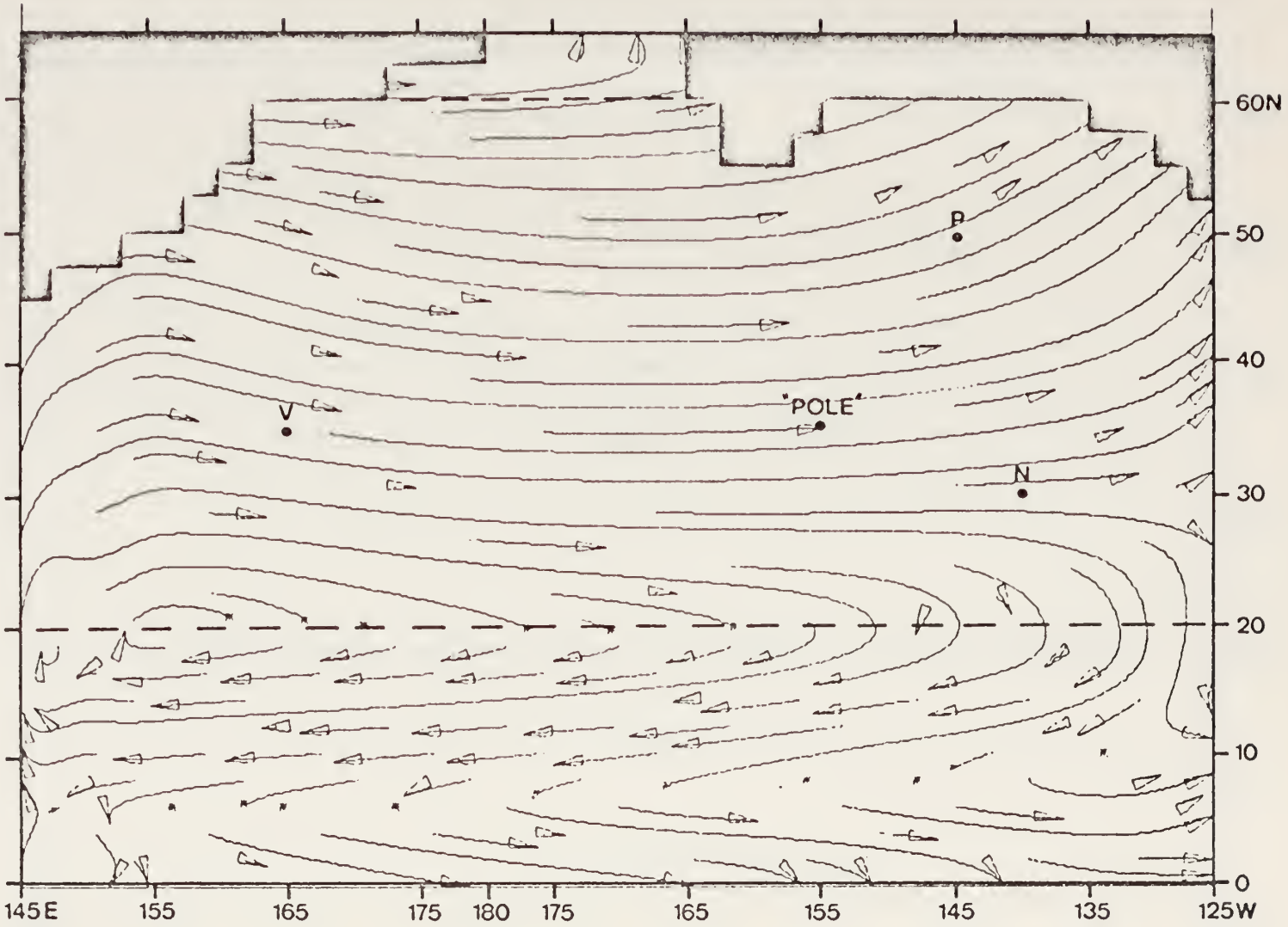

Figure 8. 30-day normal currents.

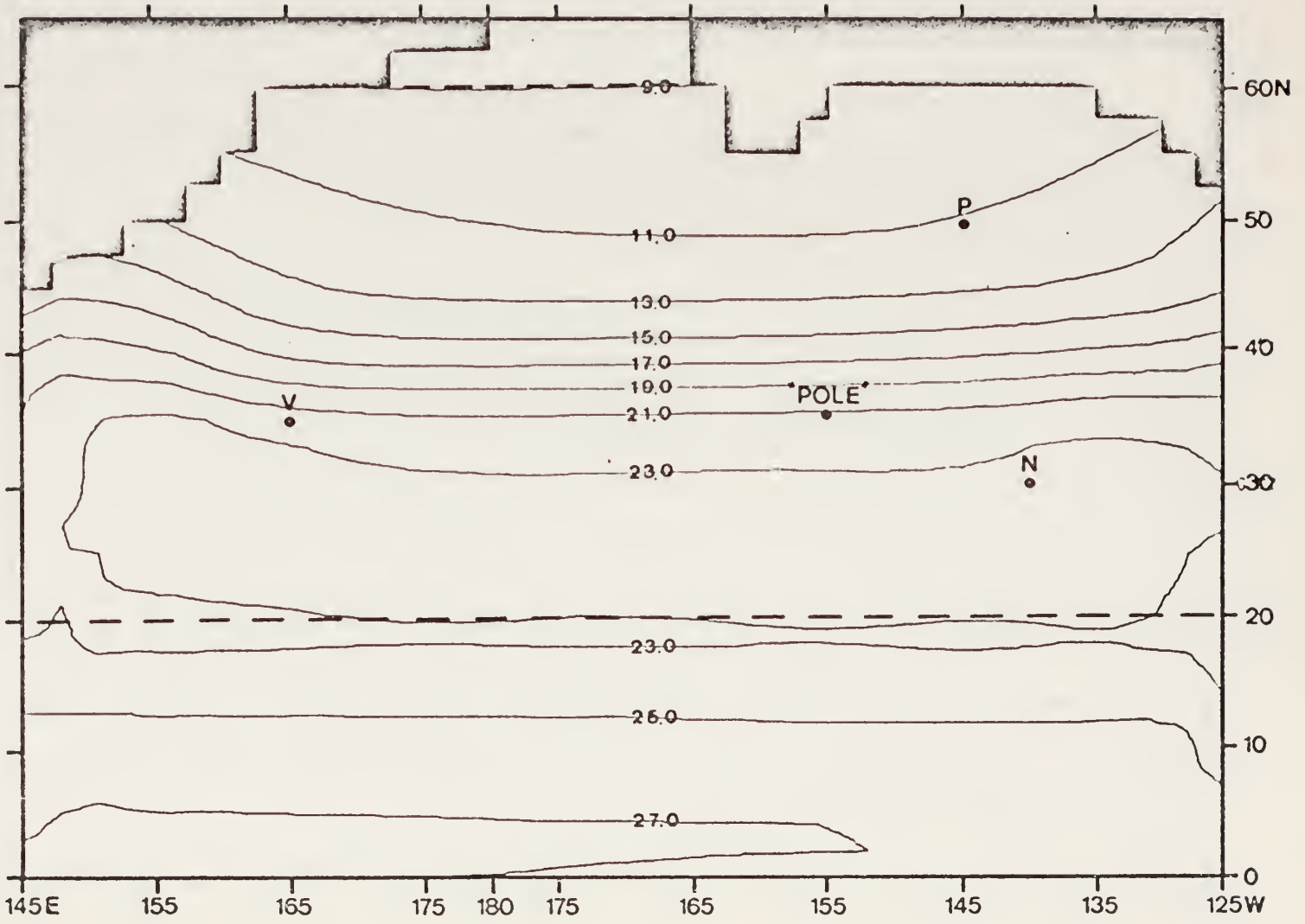

Figure 9. 30-day normal temperature field.

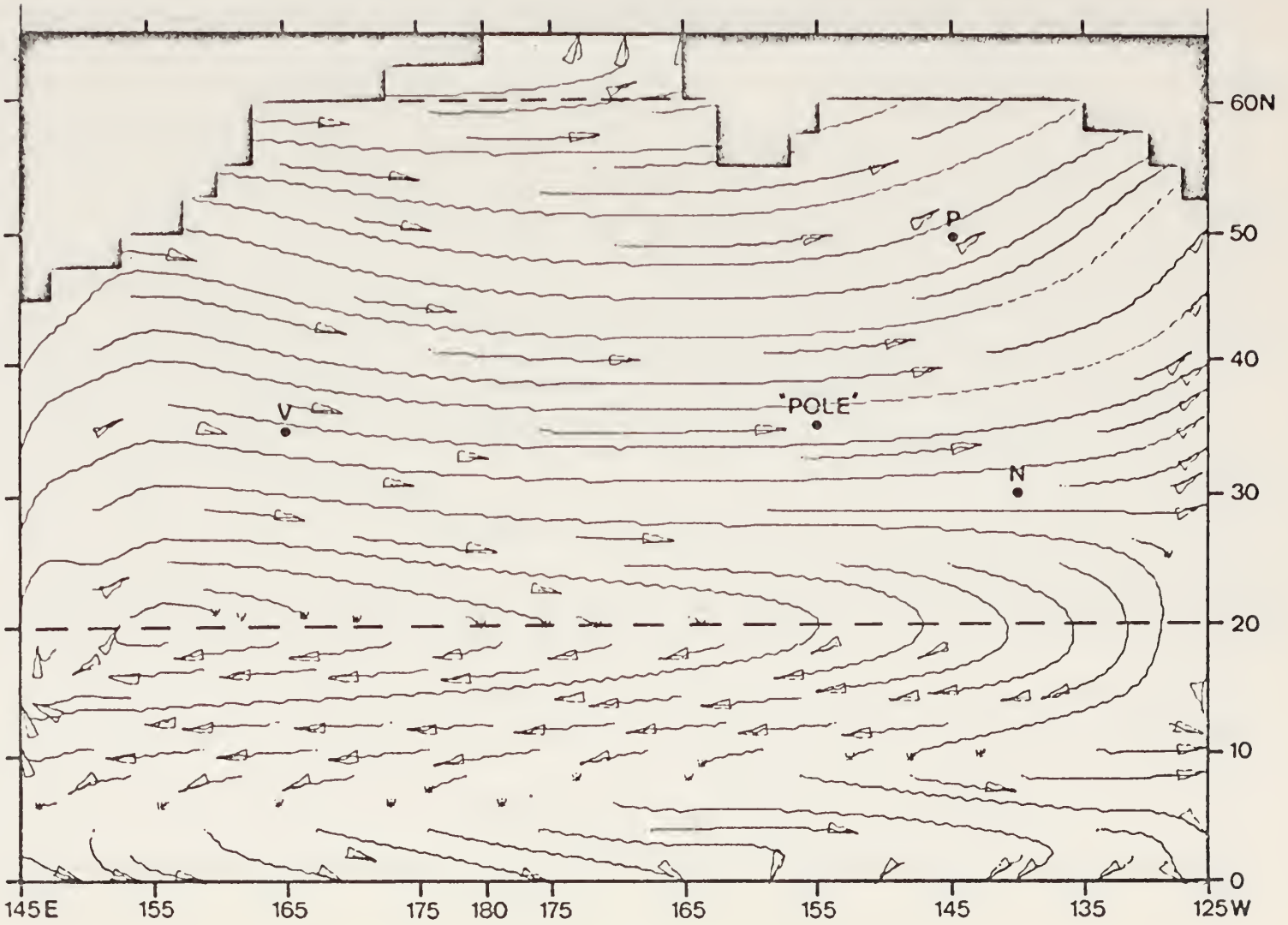

Figure 10. 60-day normal currents.

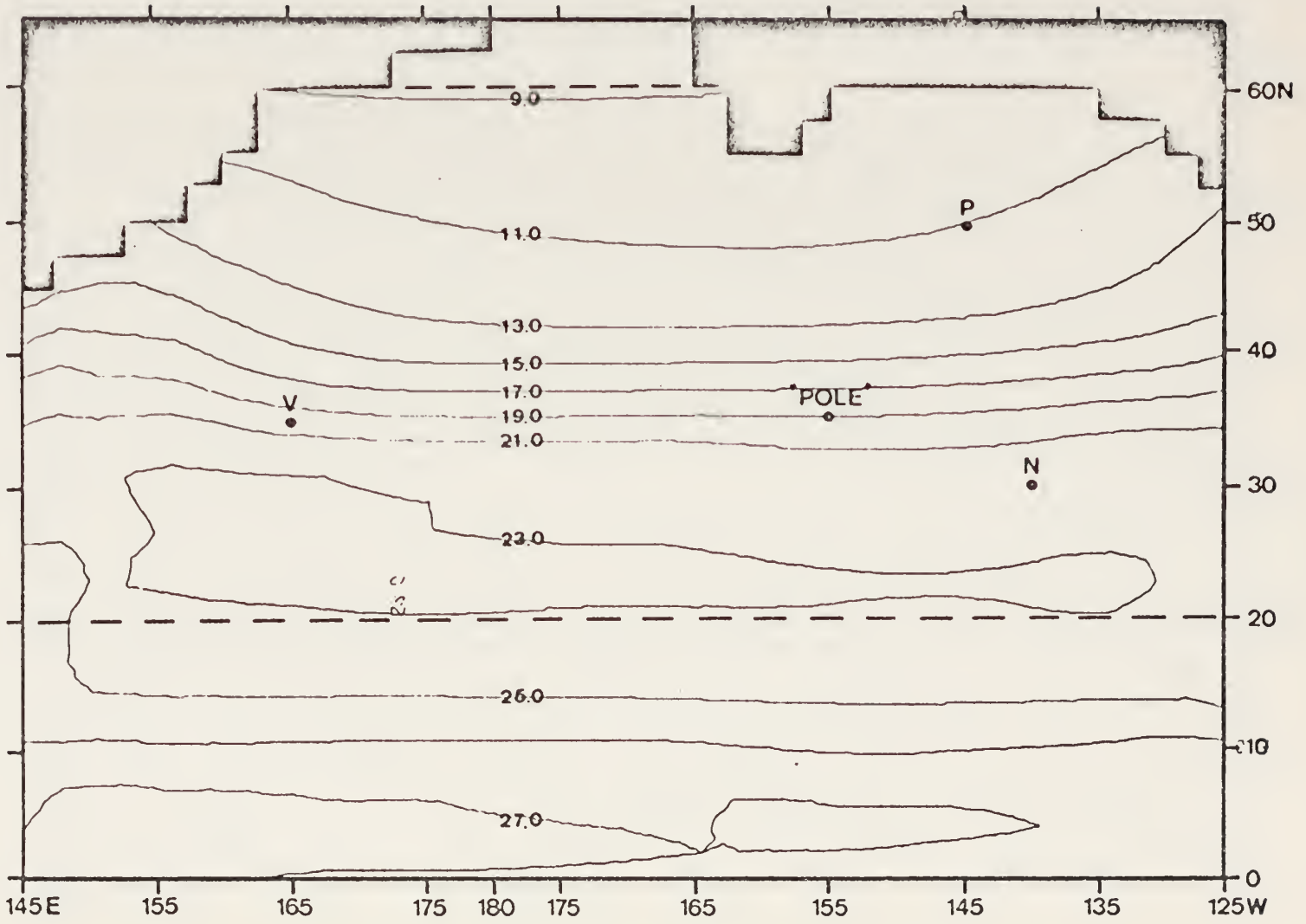

Figure 11. 60-day normal temperature field.

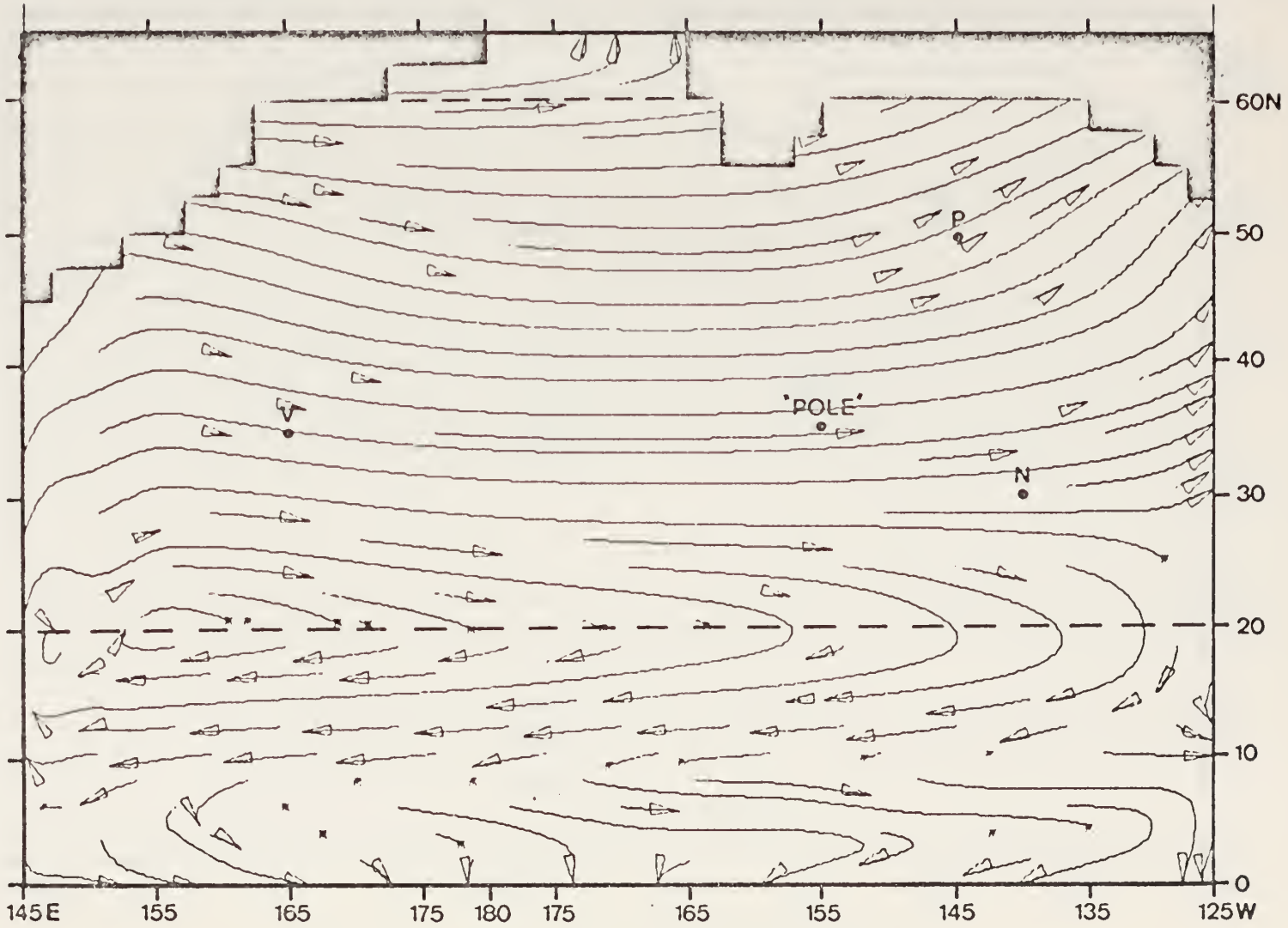

Figure 12. 90-day normal currents.

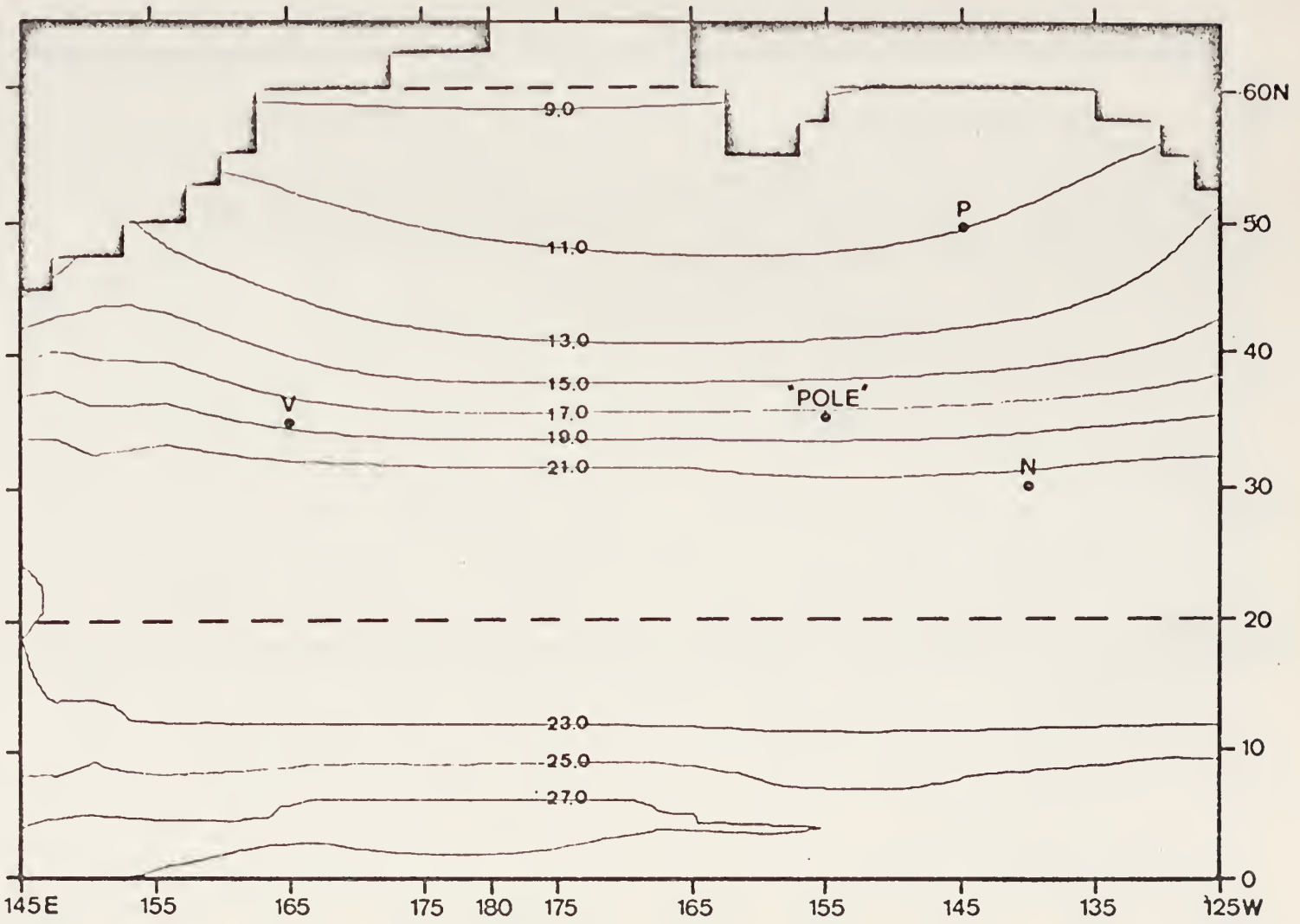

Figure 13. 90-day normal temperature field.

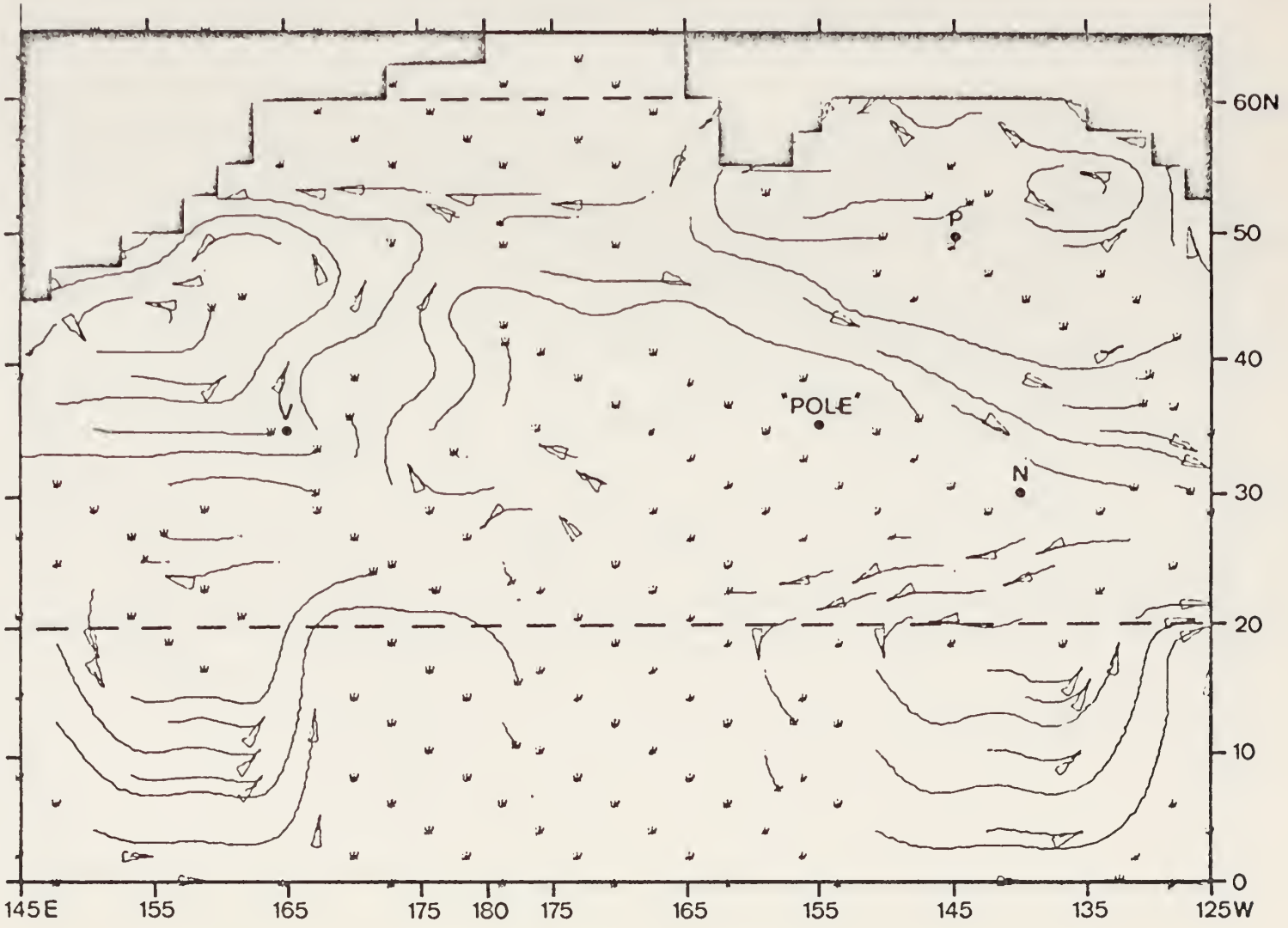

Figure 14. Initial observed anomalous currents, Fall 1971.

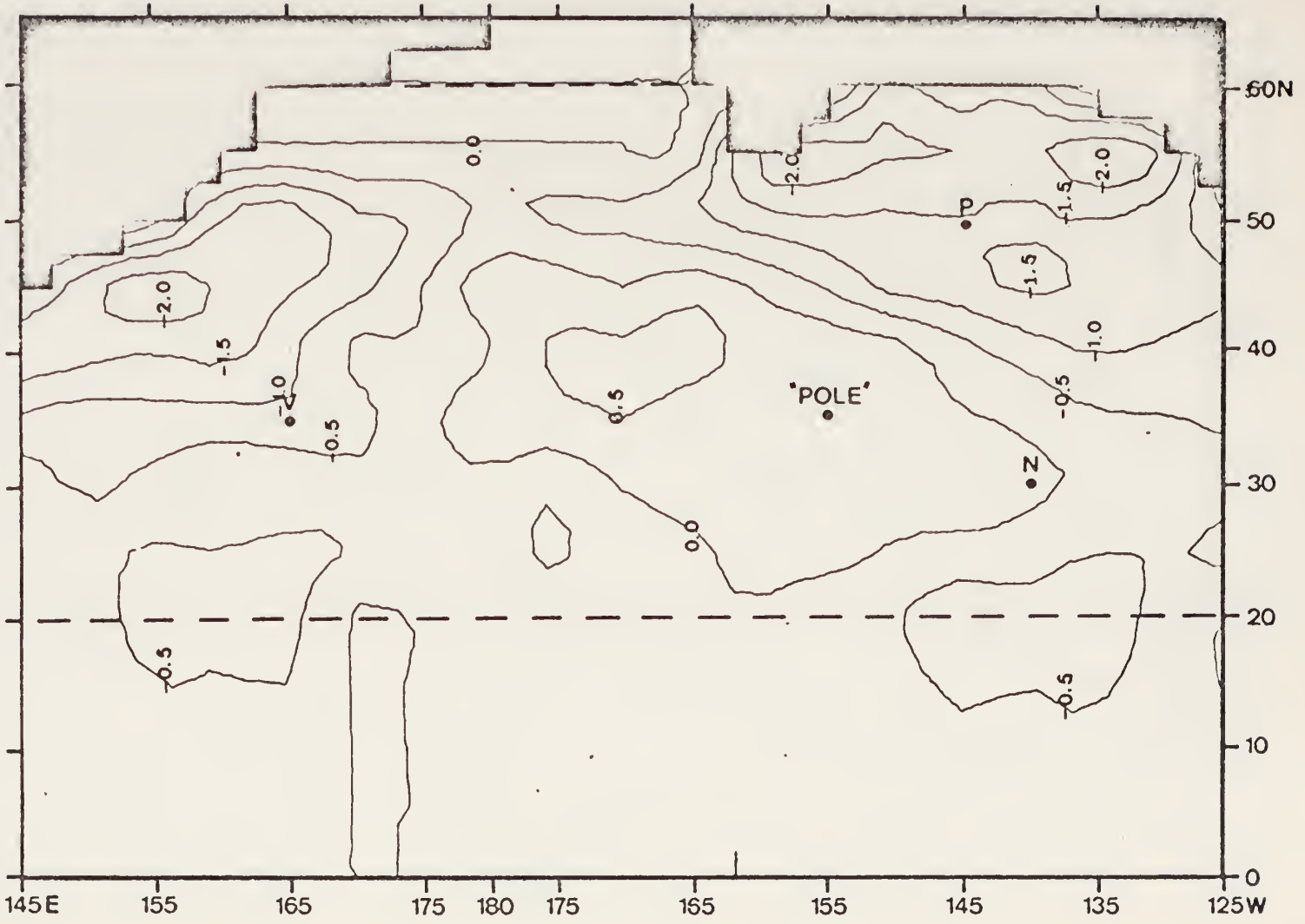

Figure 15. Initial observed anomalous temperature field, Fall 1971.

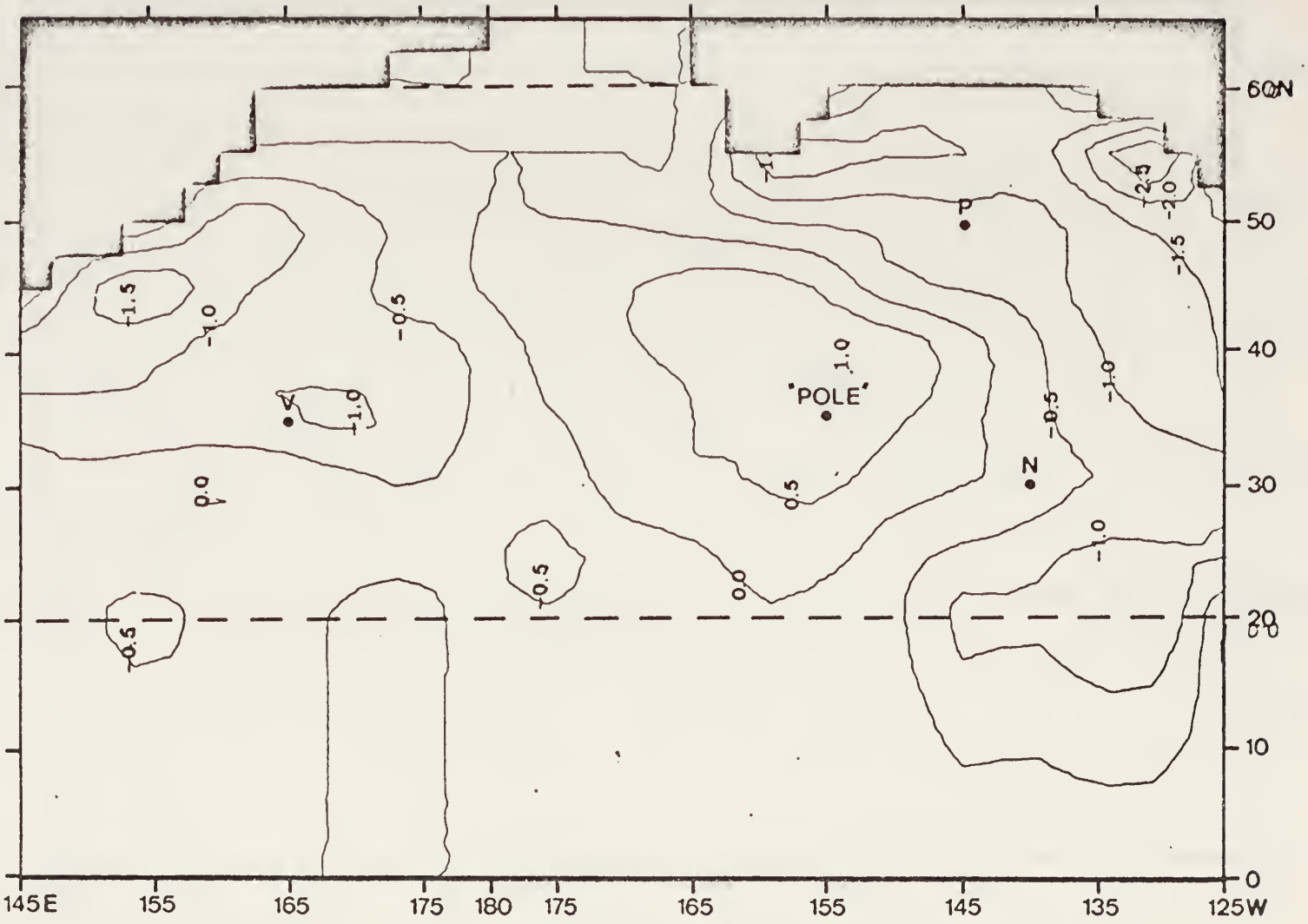

Figure 16. 30-day observed anomalous temperature field.

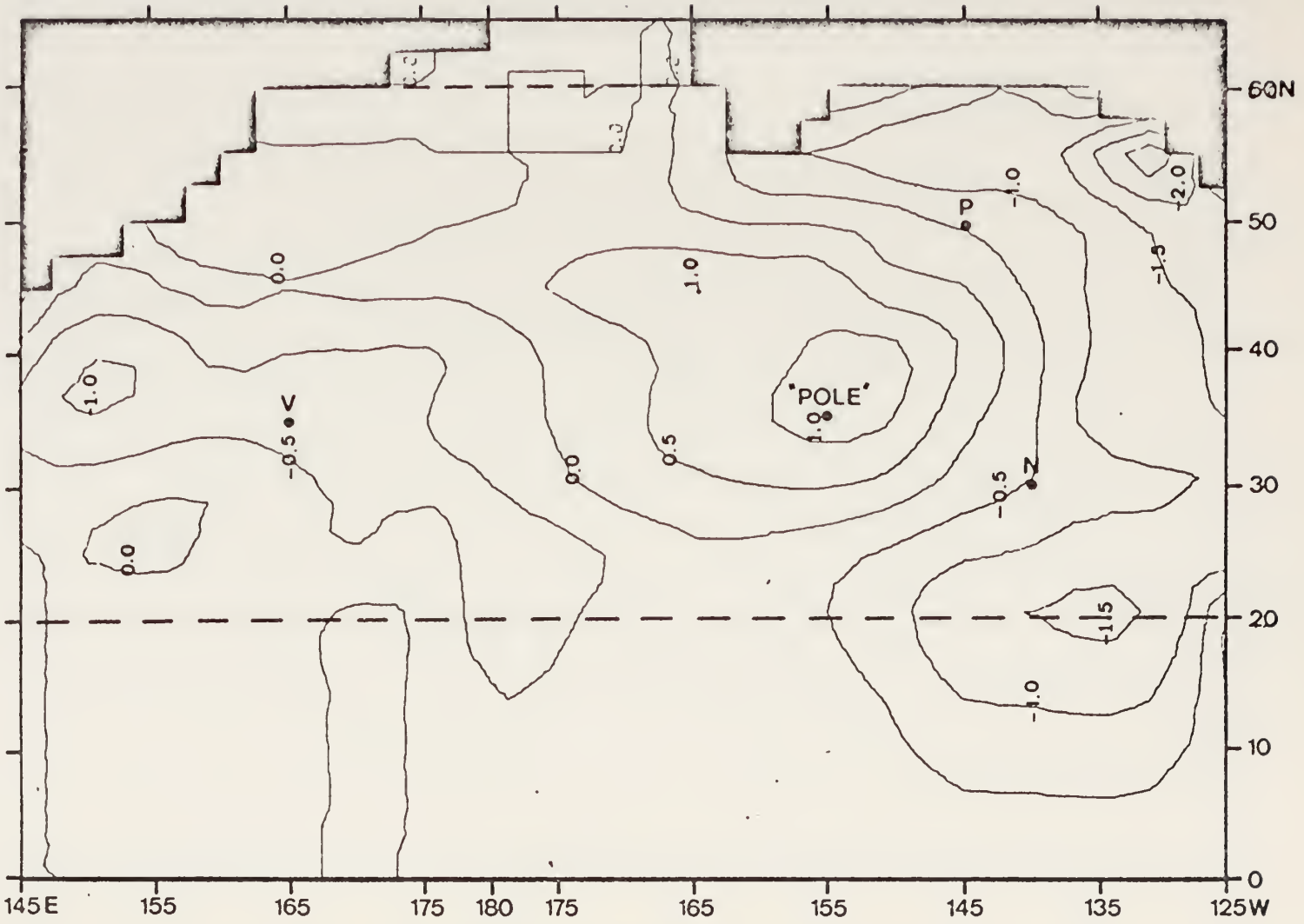

Figure 17. 60-day observed anomalous temperature field.

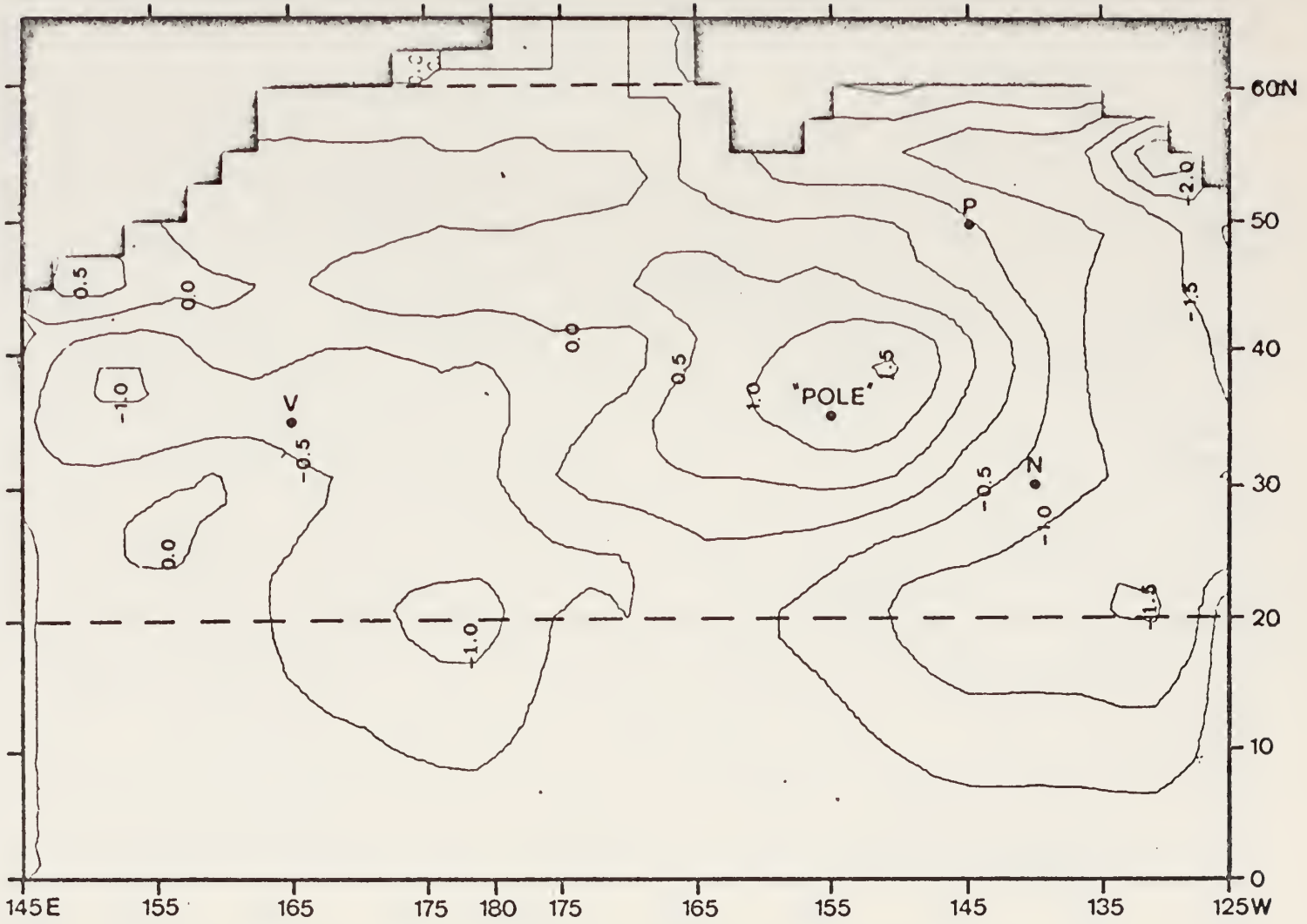

Figure 18. 90-day observed anomalous temperature field.

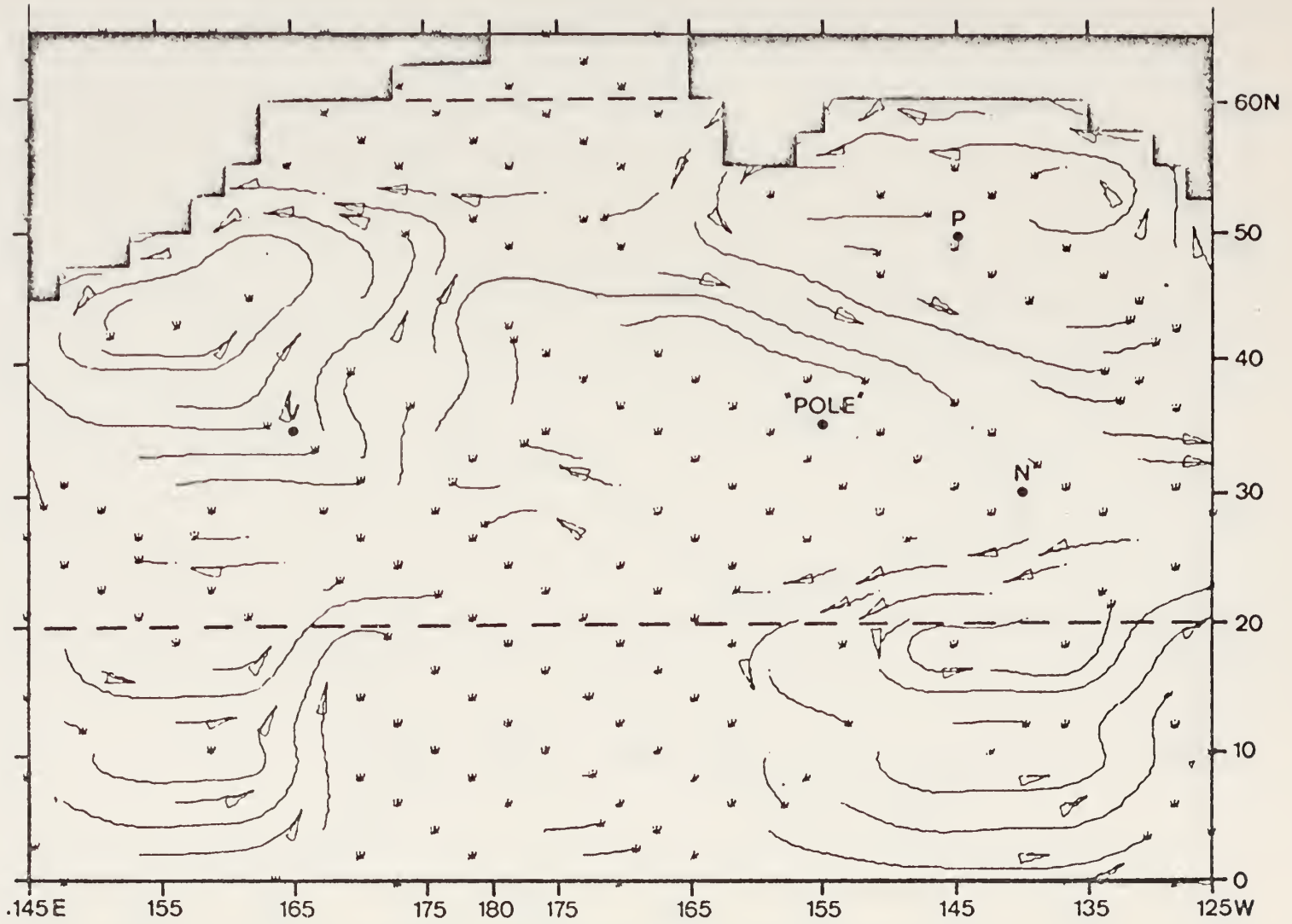

Figure 19. CASE 1: 30-day predicted anomalous currents.

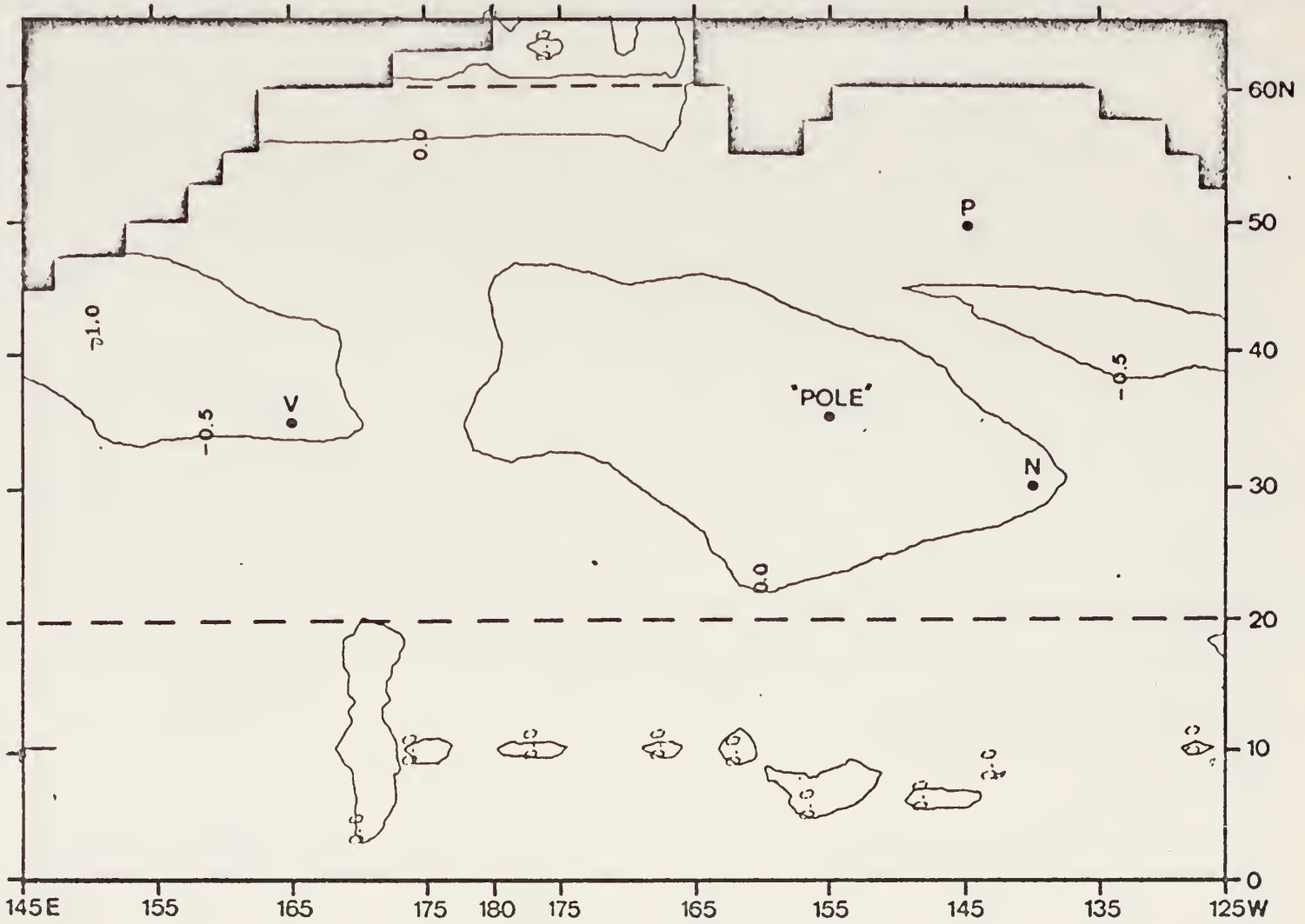

Figure 20. CASE 1: 30-day predicted anomalous temperature field.

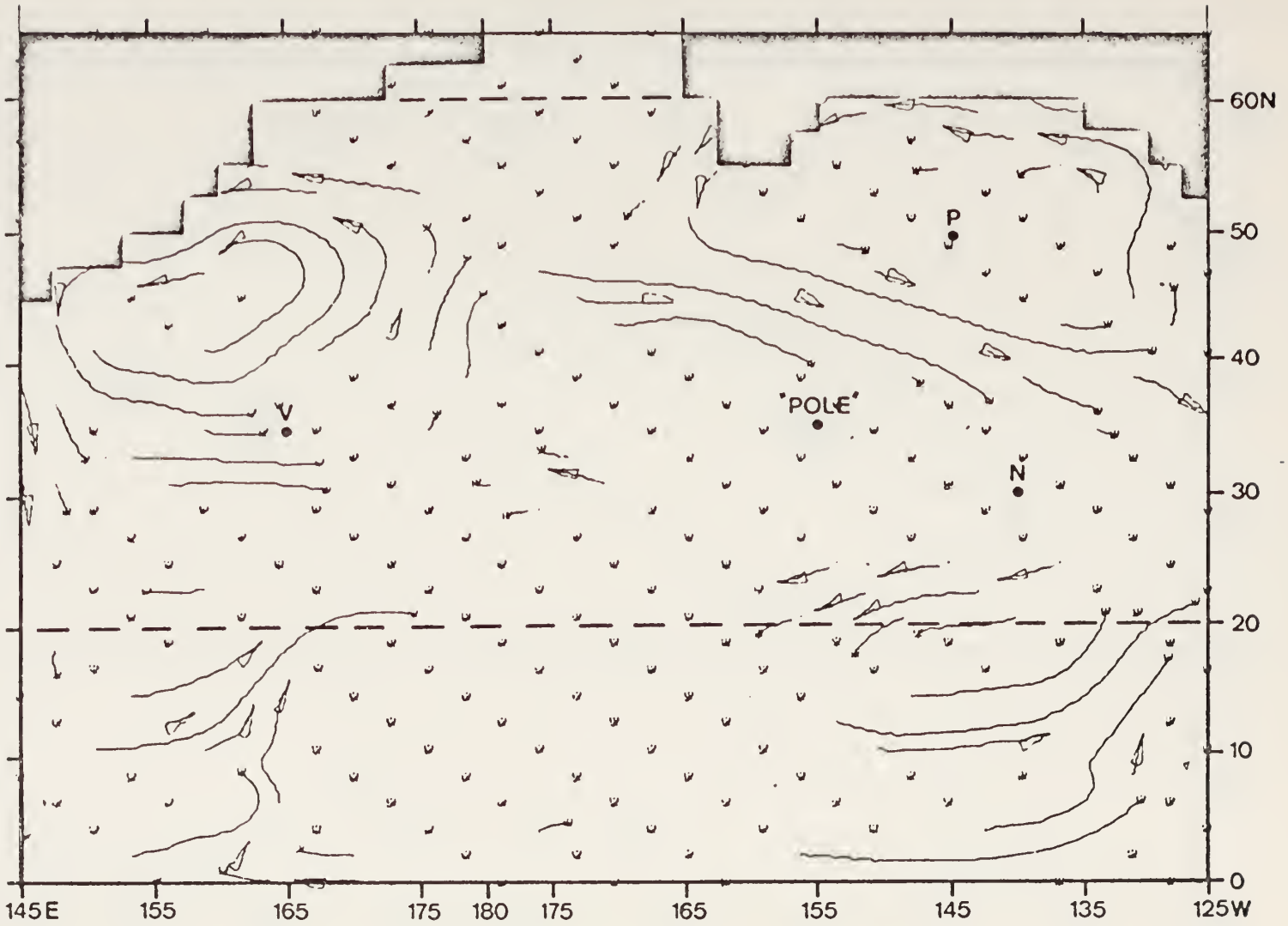

Figure 21. CASE 1: 60-day predicted anomalous currents.

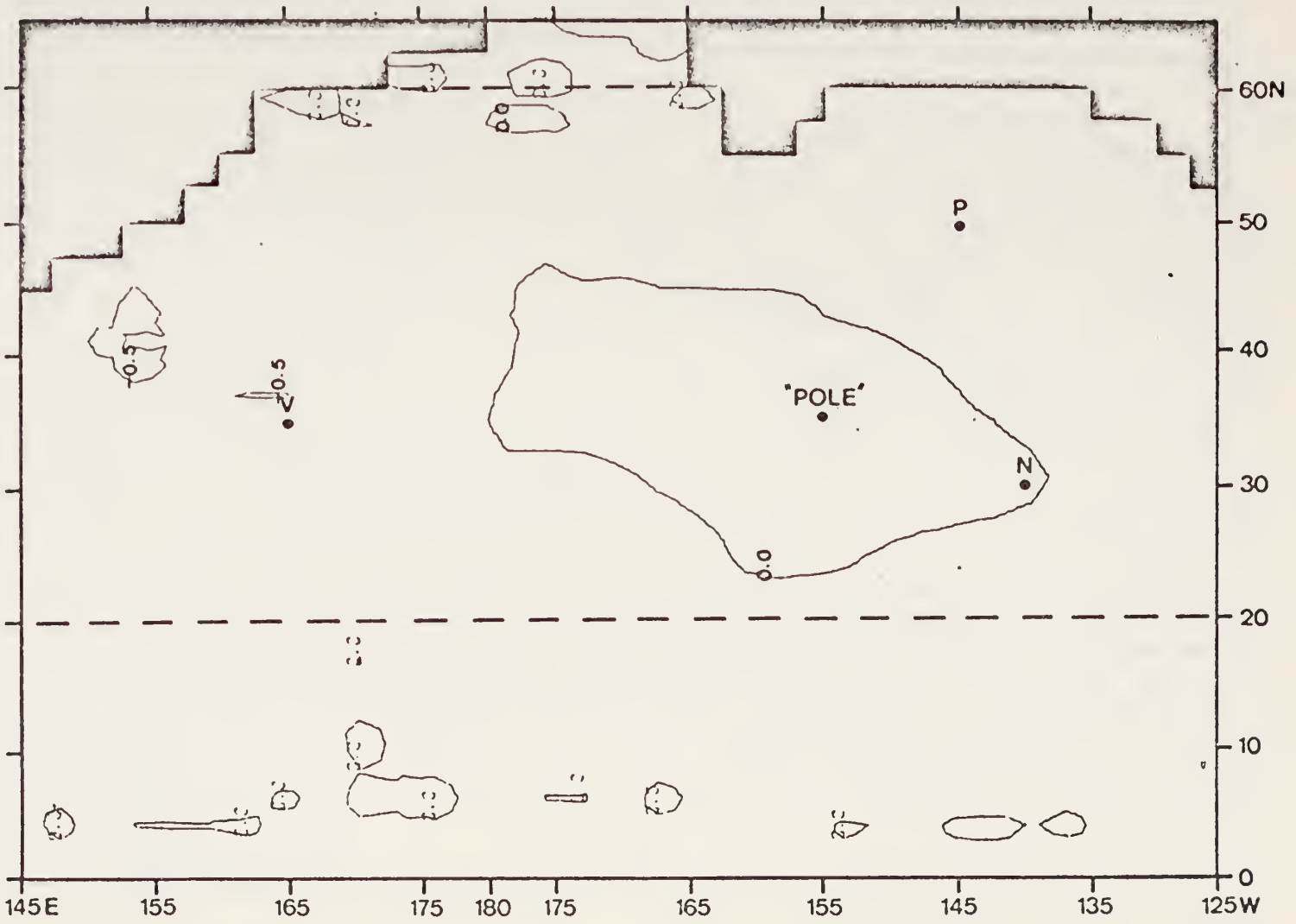

Figure 22. CASE 1: 60-day predicted anomalous temperature field.

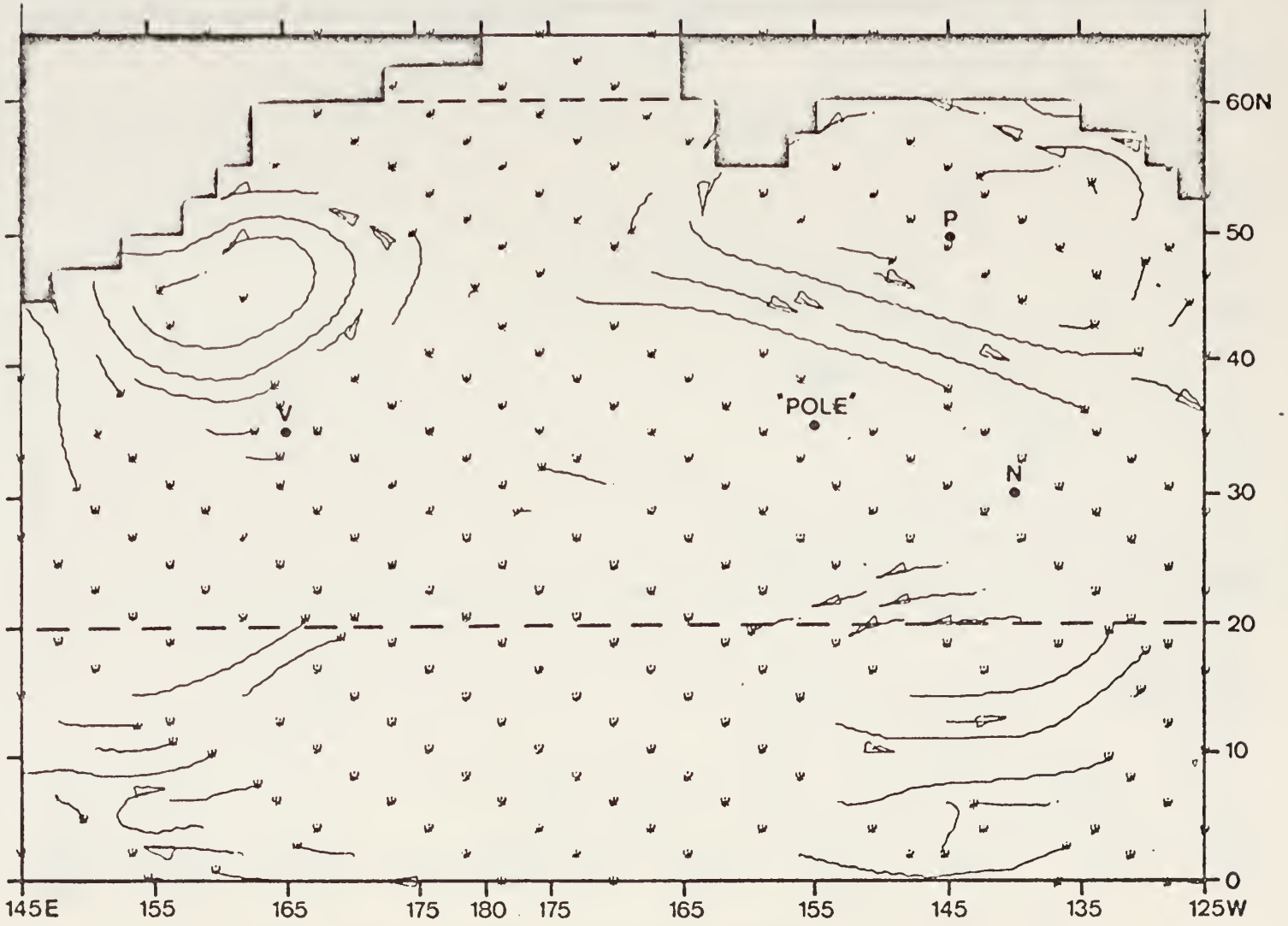

Figure 23. CASE 1: 90-day predicted anomalous currents.

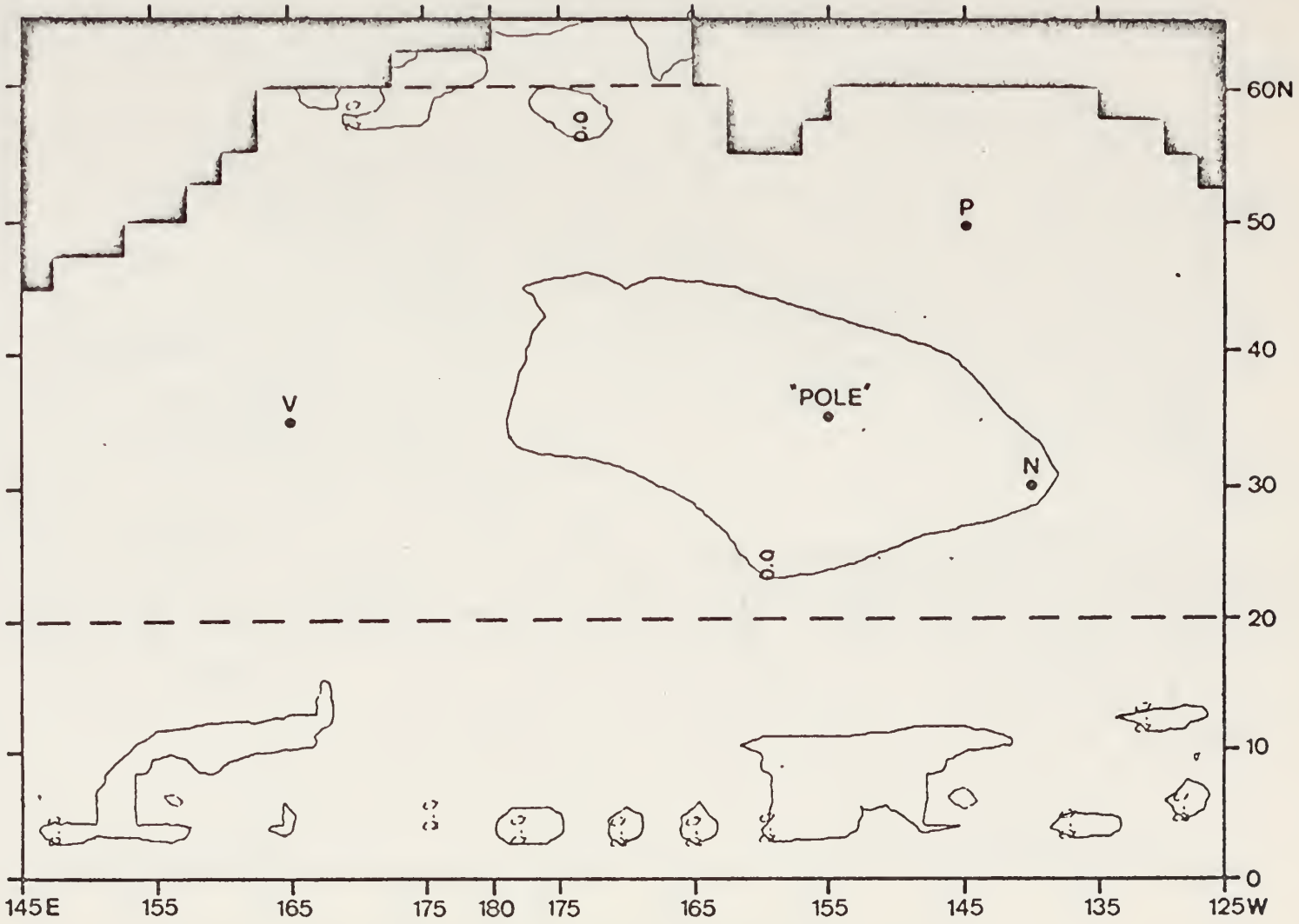

Figure 24. CASE 1: 90-day predicted anomalous temperature field.

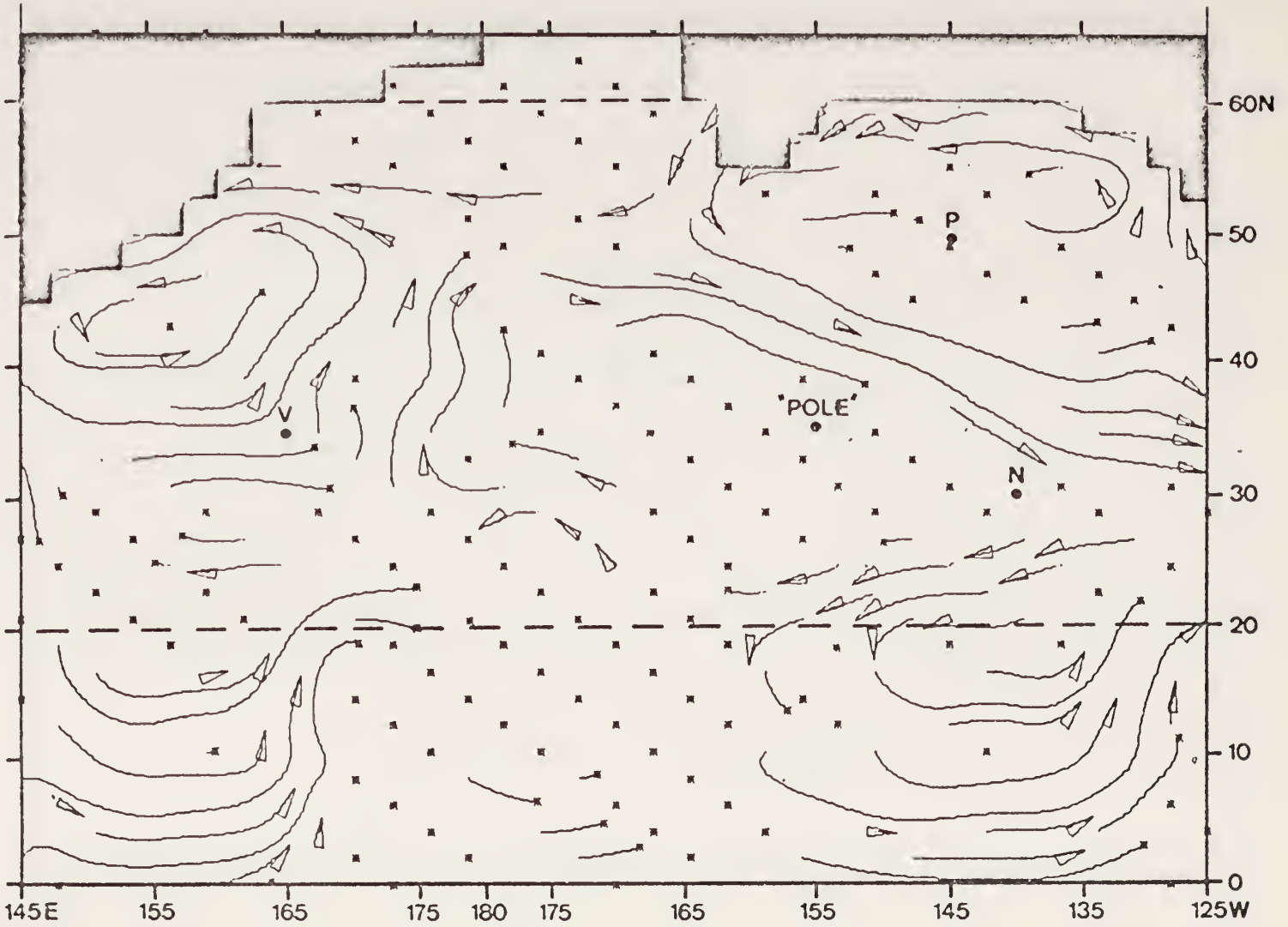

Figure 25. CASE 2: 30-day predicted anomalous currents.

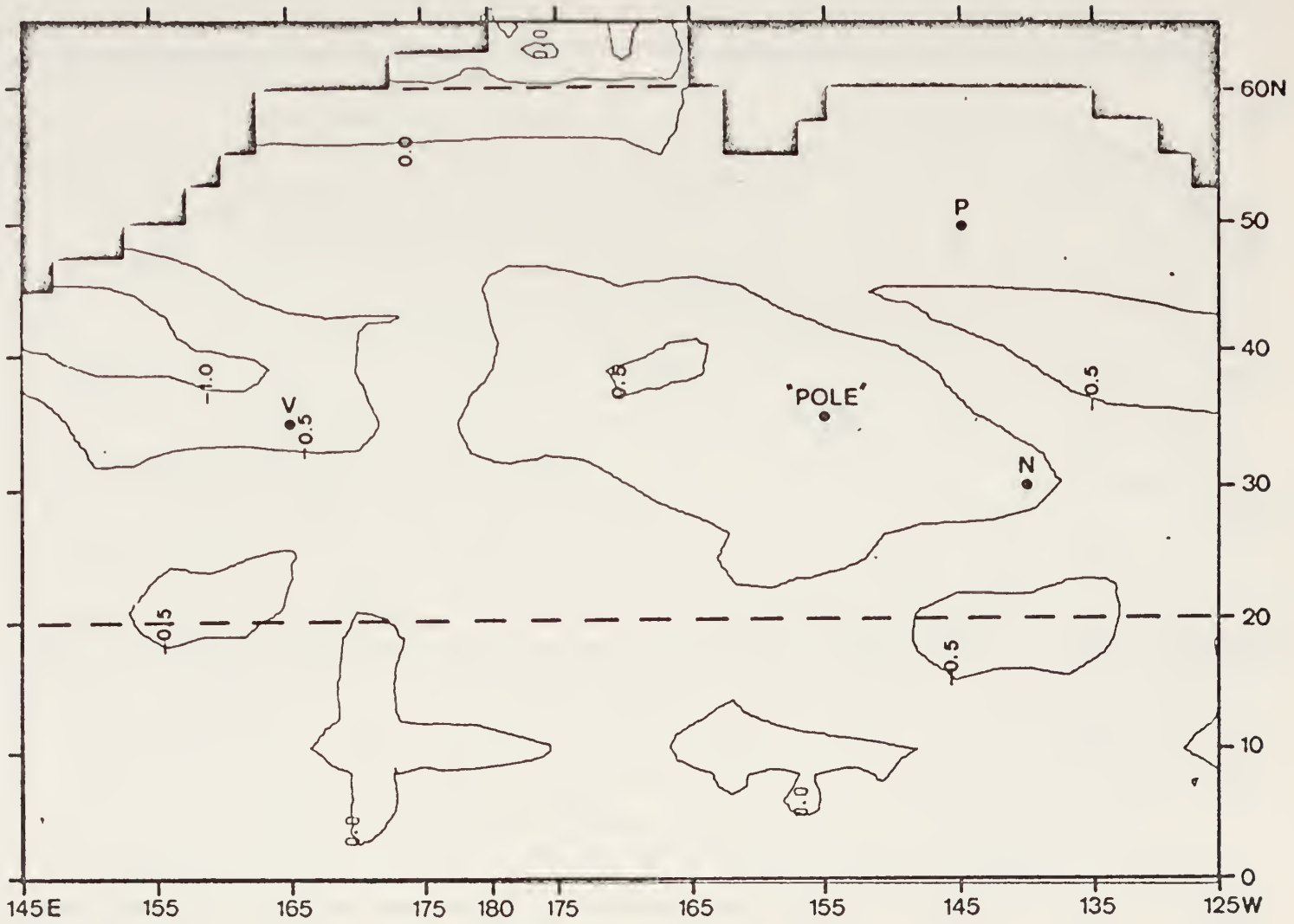

Figure 26. CASE 2: 30-day predicted anomalous temperature field.

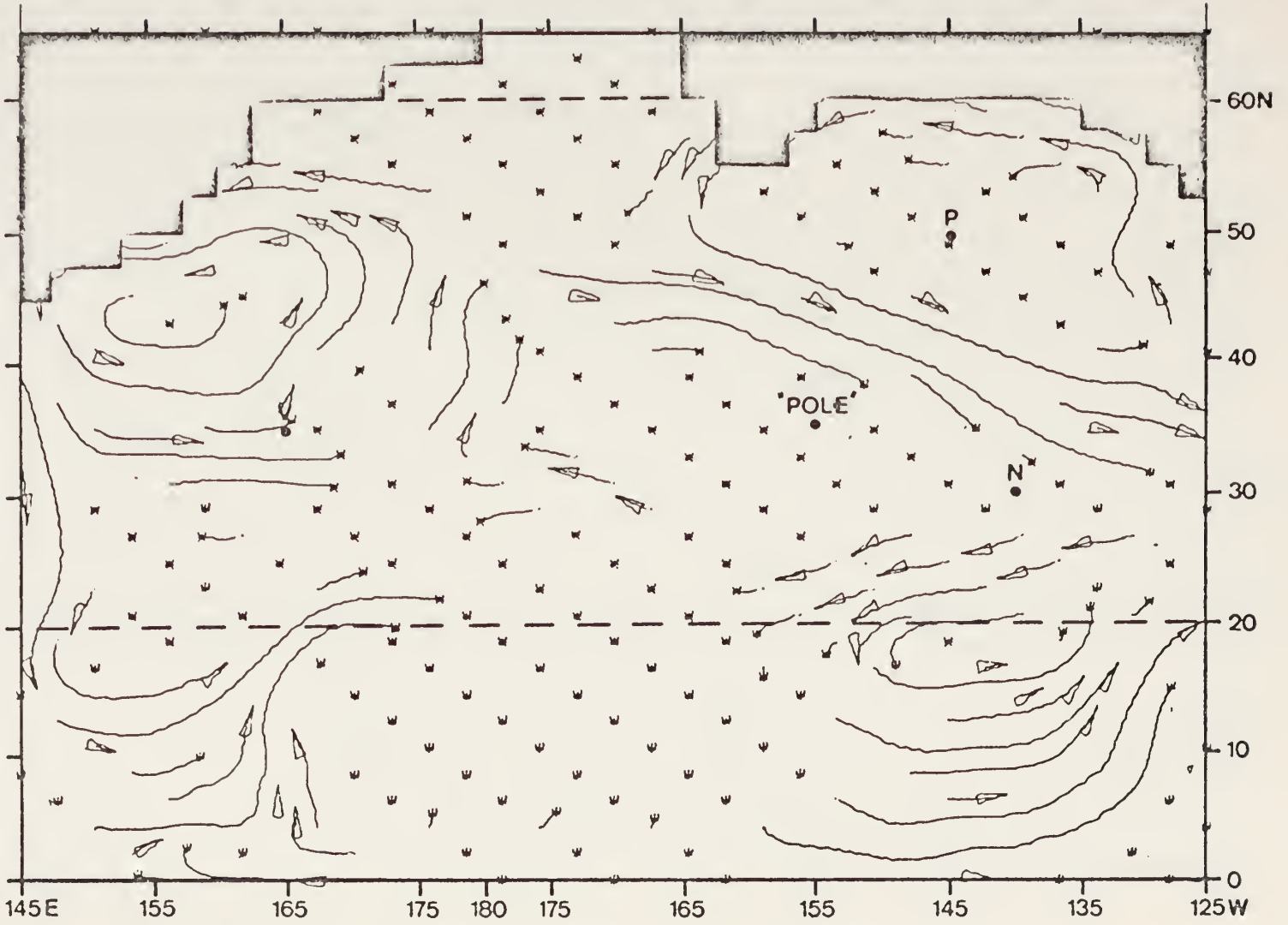

Figure 27. CASE 2: 60-day predicted anomalous currents.

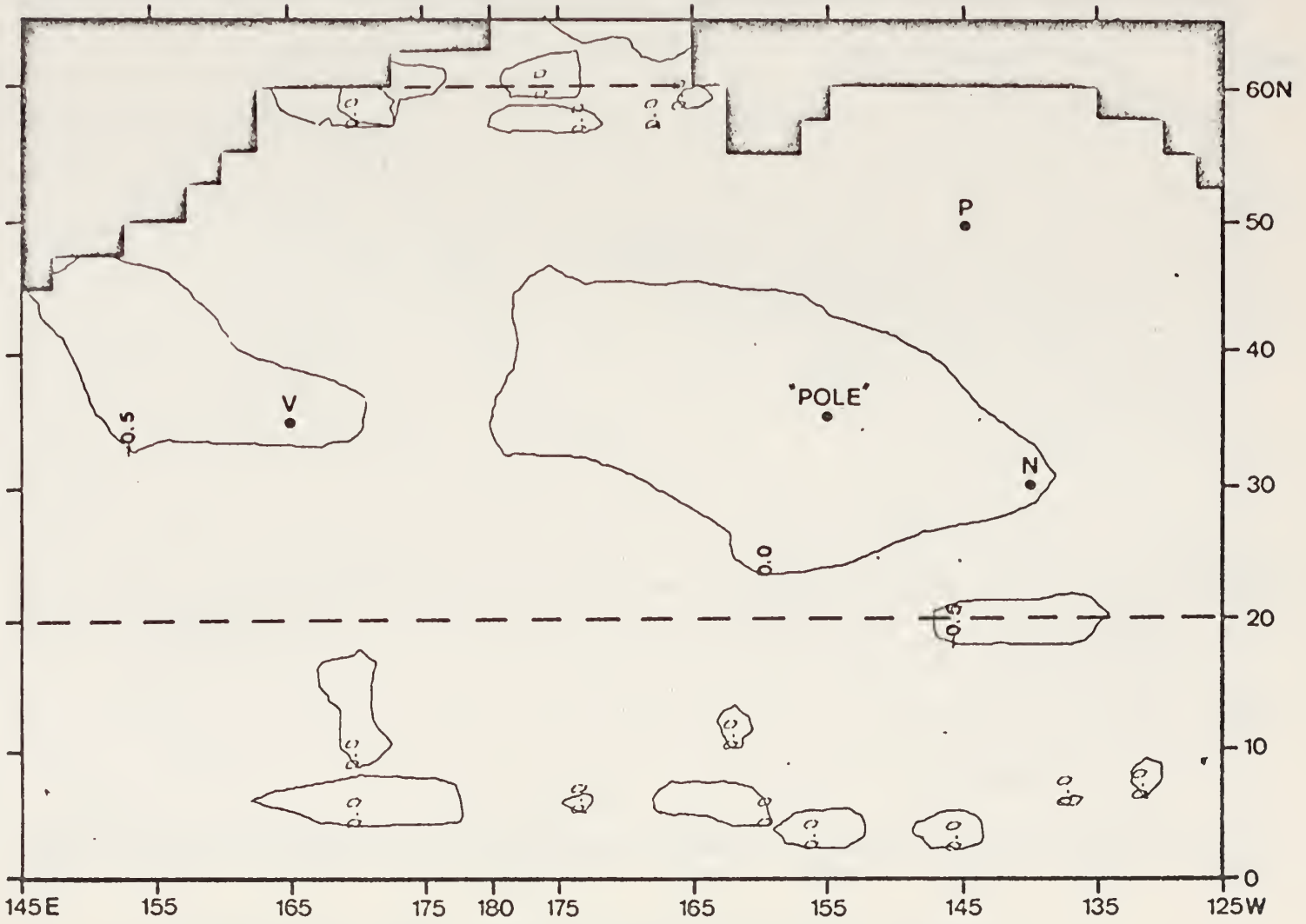

Figure 28. CASE 2: 60-day predicted anomalous temperature field.

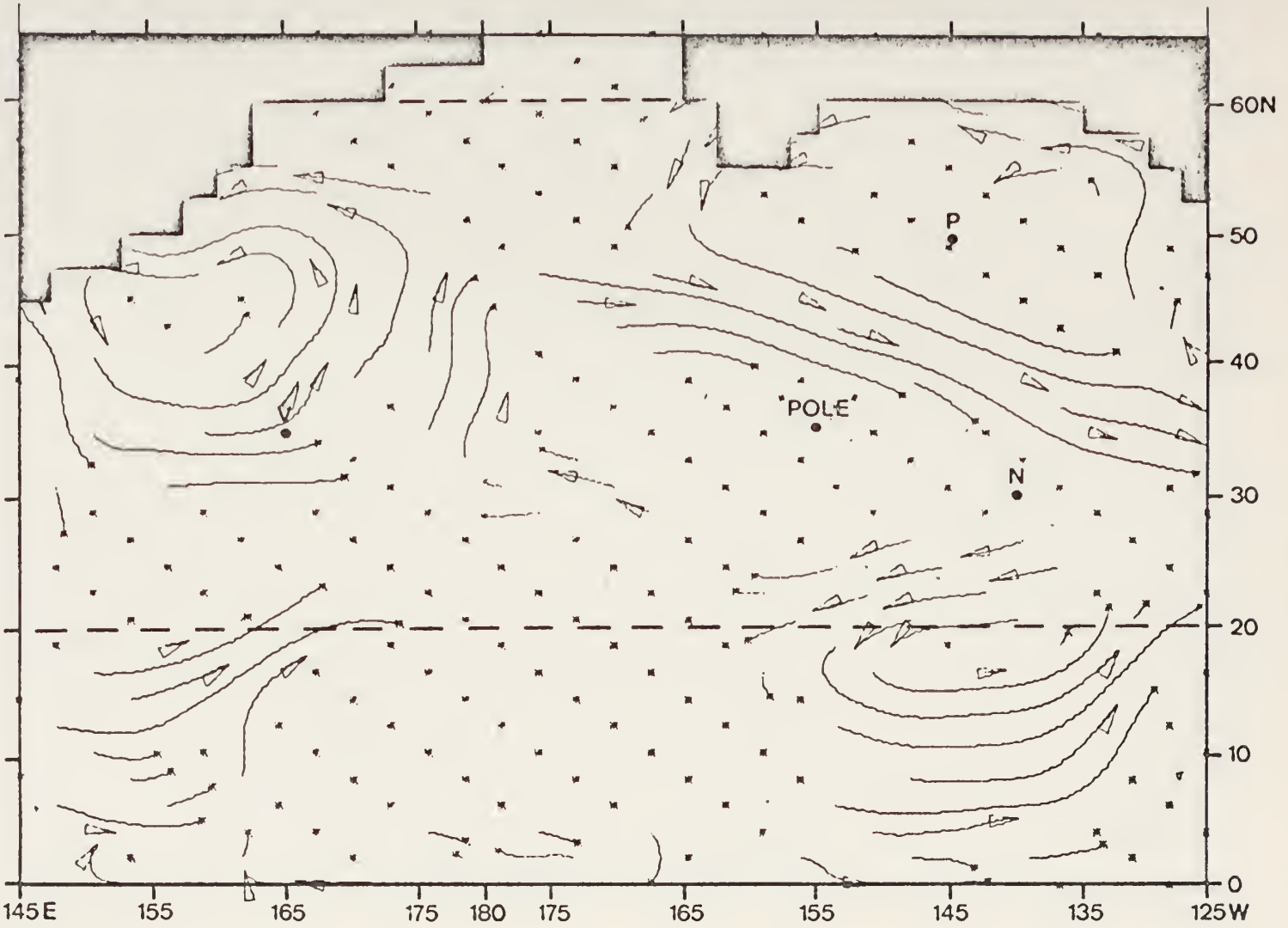

Figure 29. CASE 2: 90-day predicted anomalous currents.

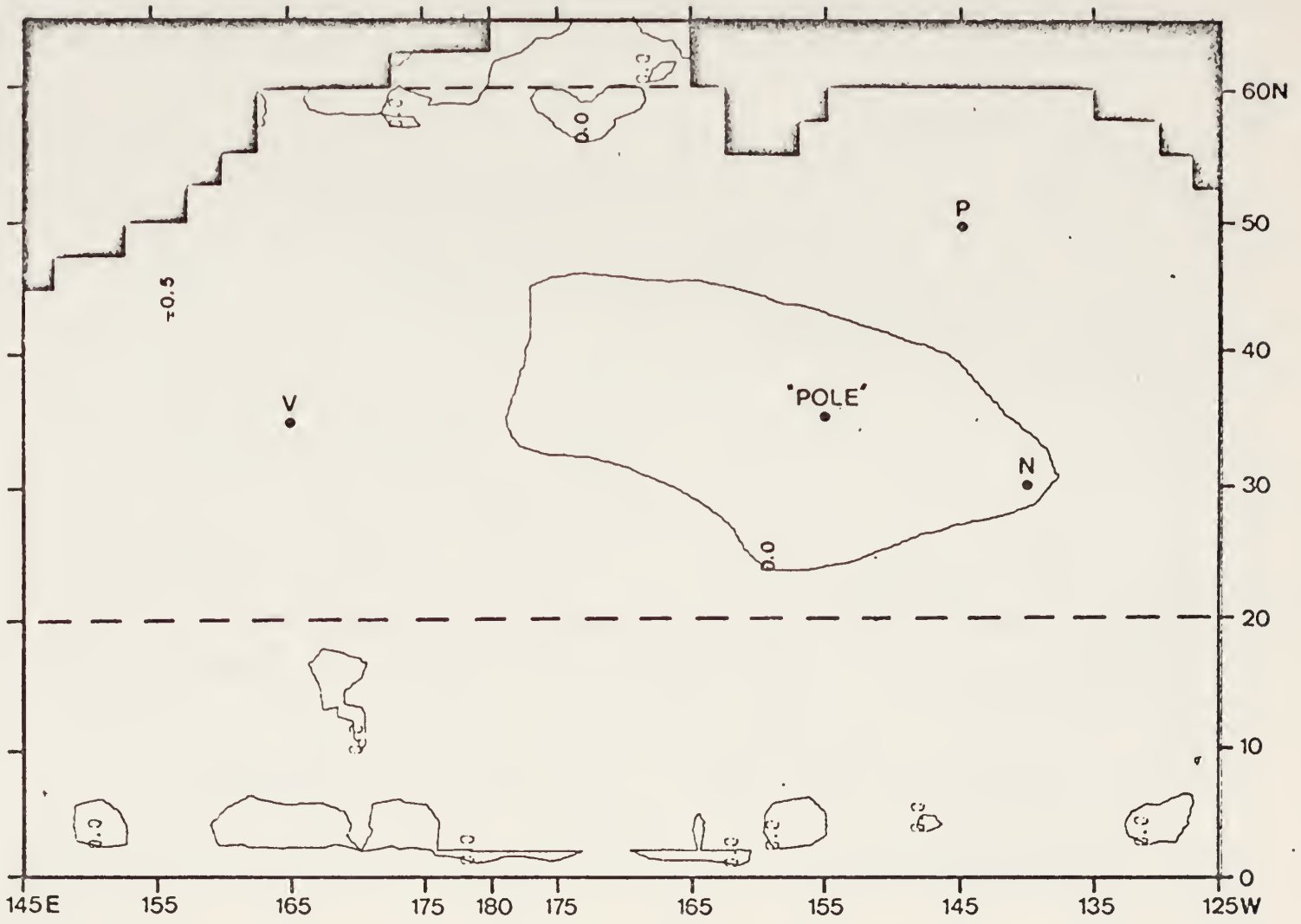

Figure 30. Case 2: 90-day predicted anomalous temperature field.

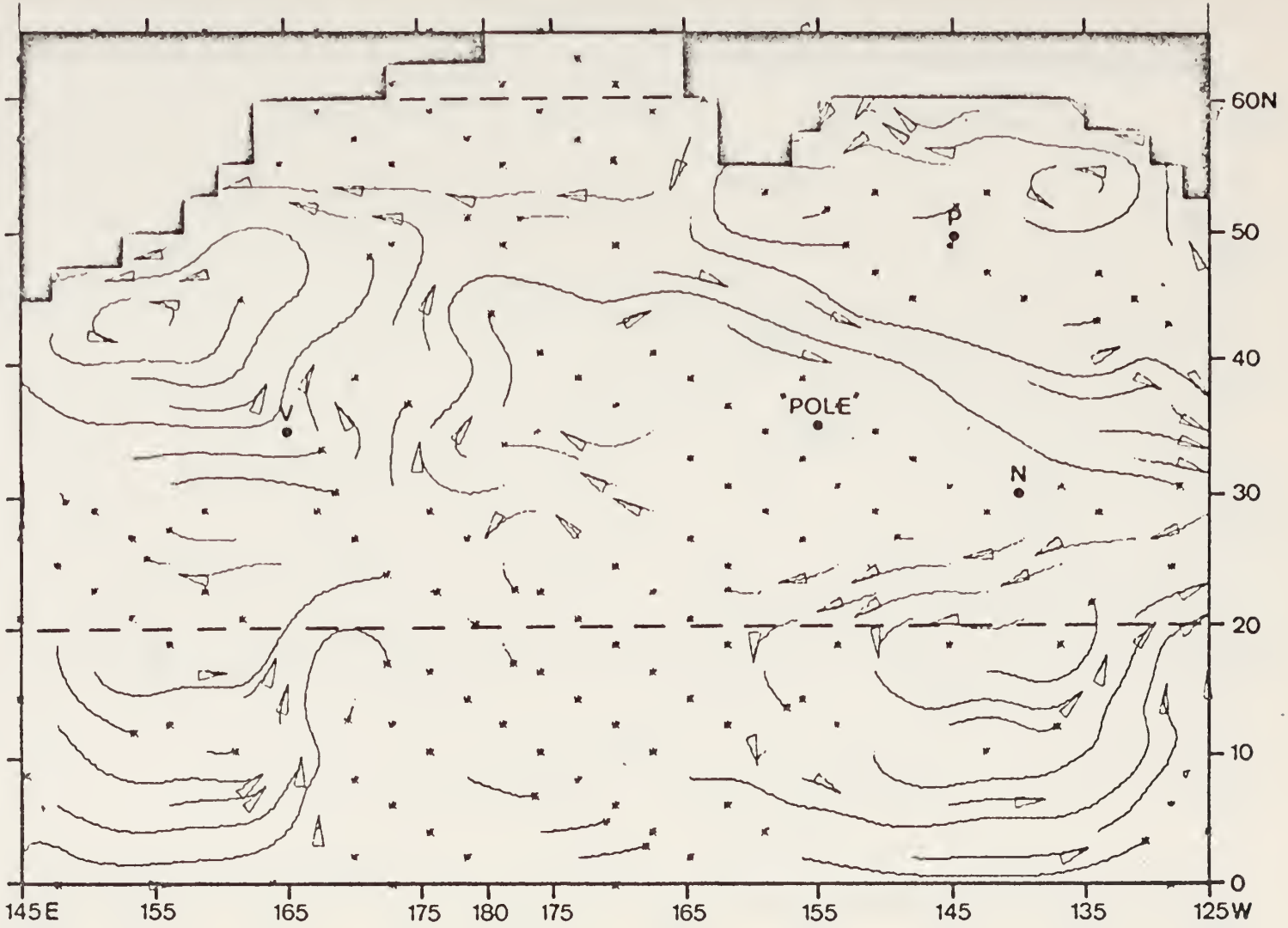

Figure 31. CASE 3: 30-day predicted anomalous currents.

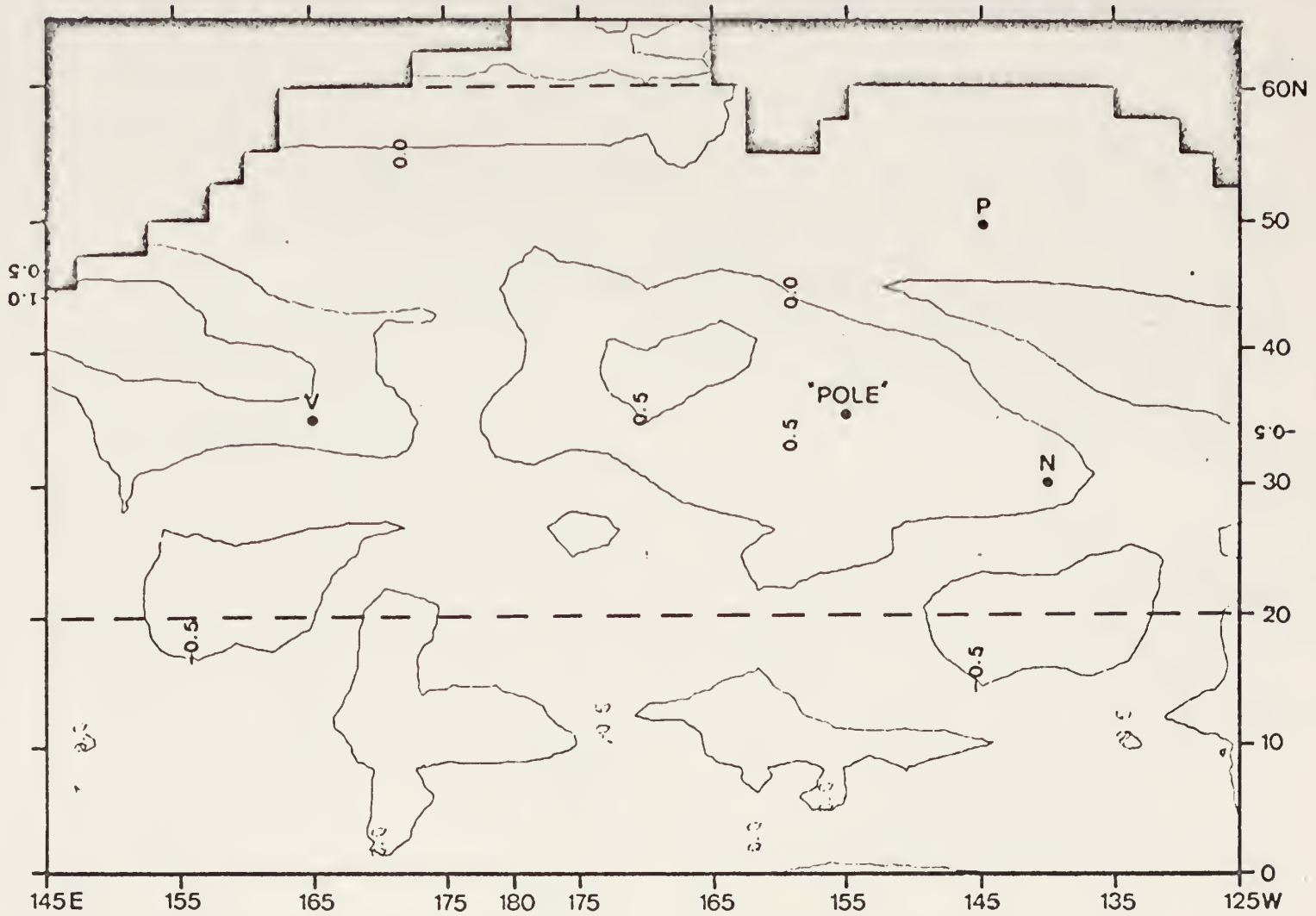

Figure 32. CASE 3: 30-day predicted anomalous temperature field.

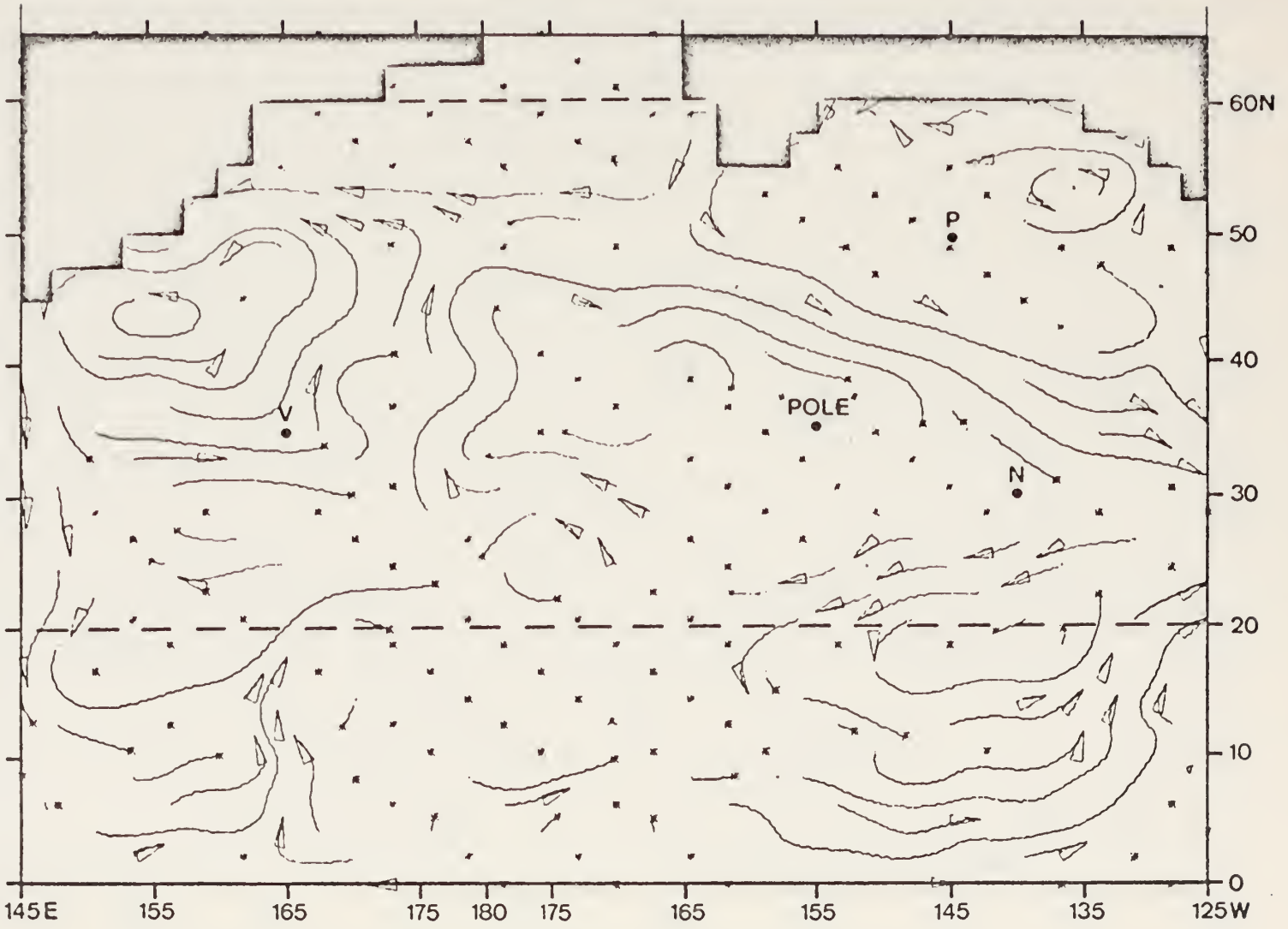

Figure 33. CASE 3: 60-day predicted anomalous currents.

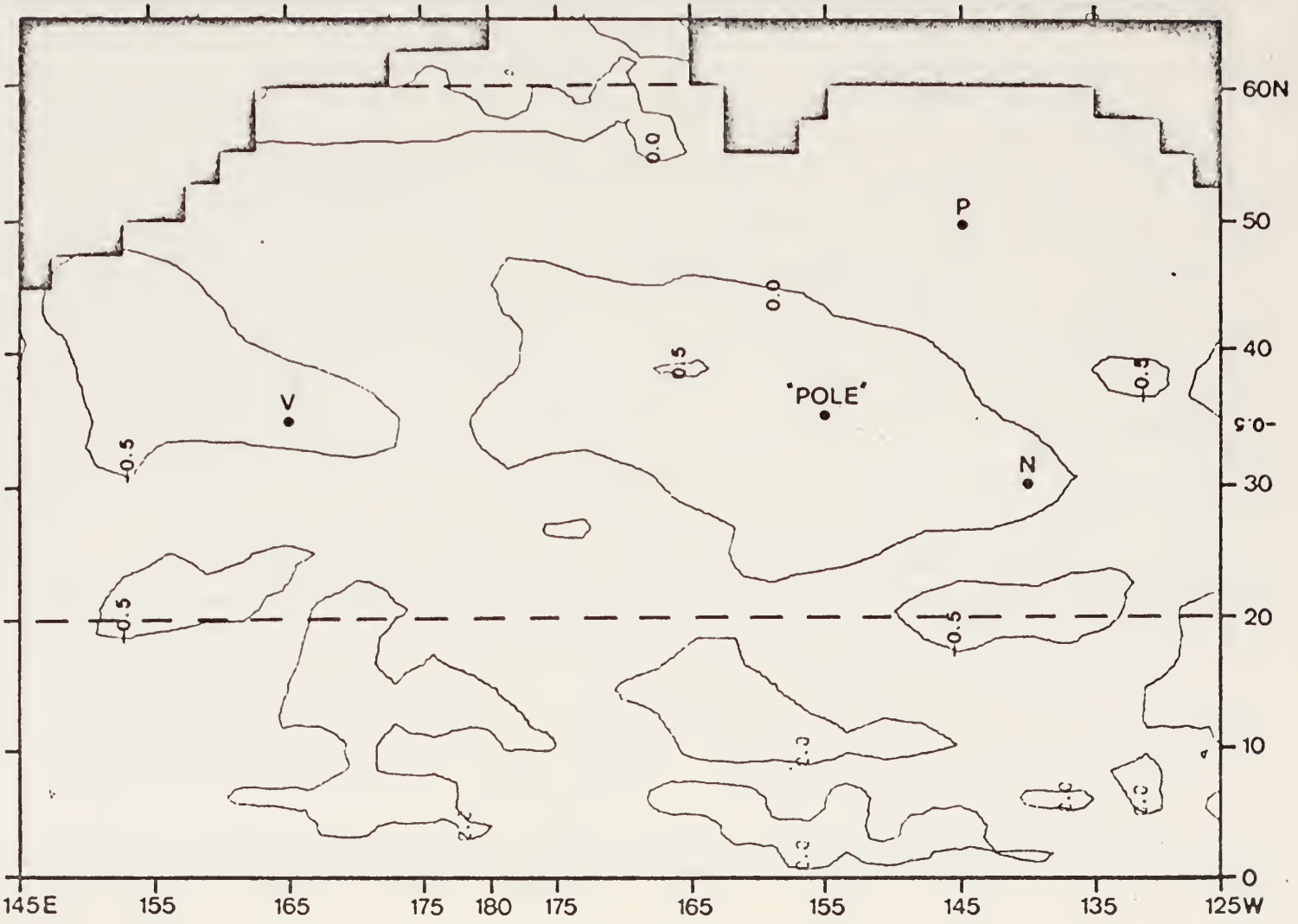

Figure 34. CASE 3: 60-day predicted anomalous temperature field.

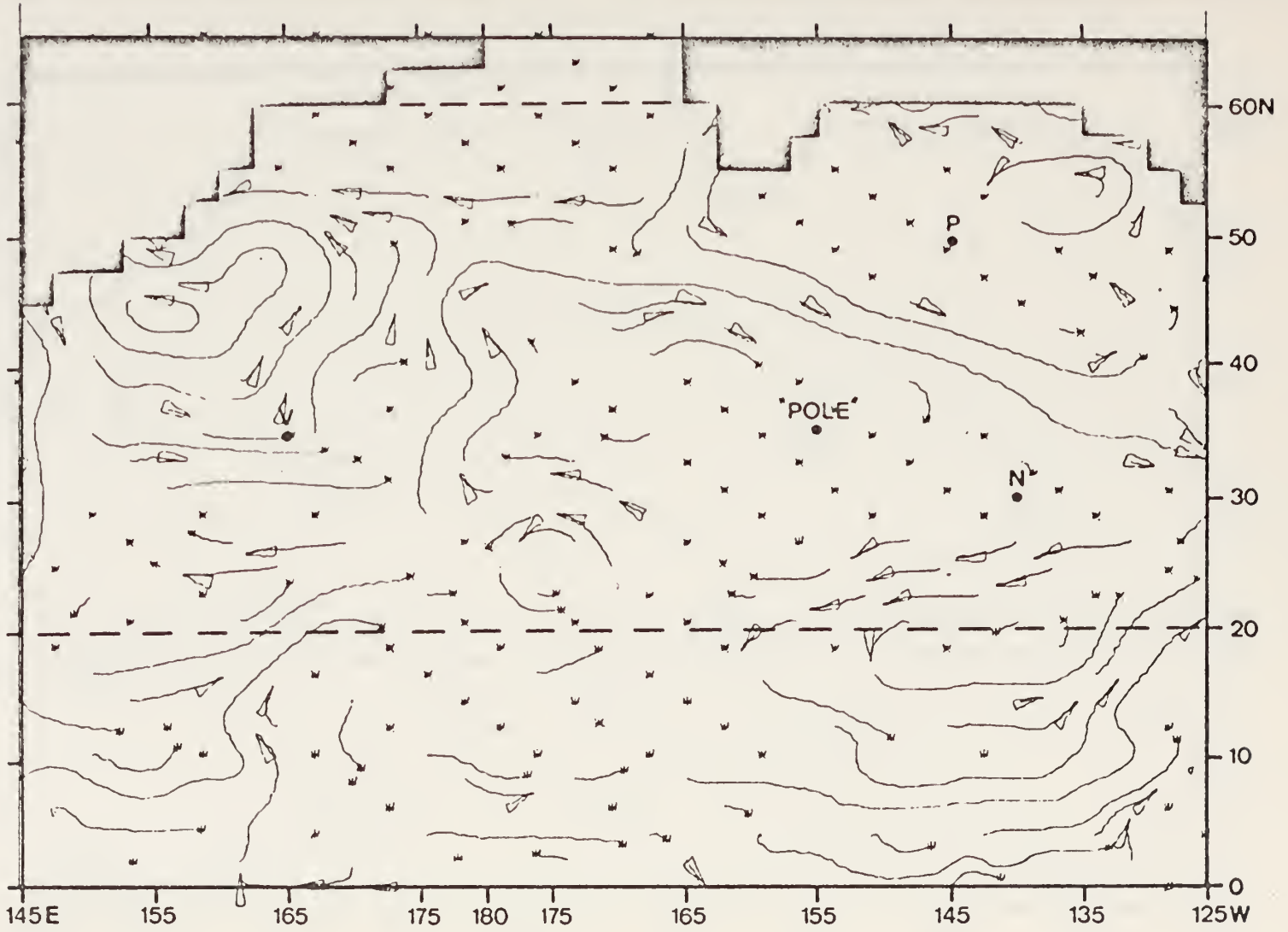

Figure 35. CASE 3: 90-day predicted anomalous currents.

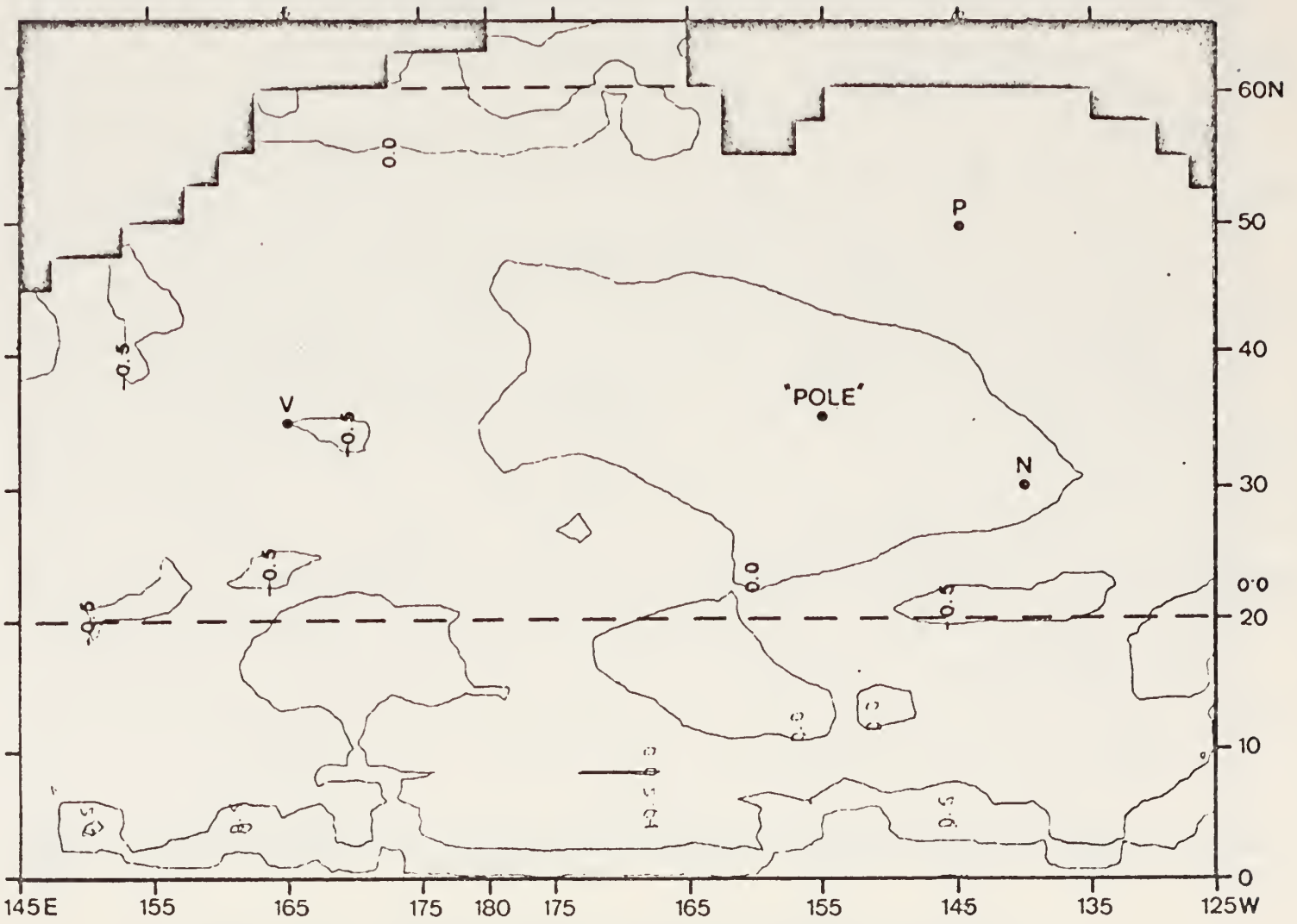

Figure 36. CASE 3: 90-day predicted anomalous temperature field.

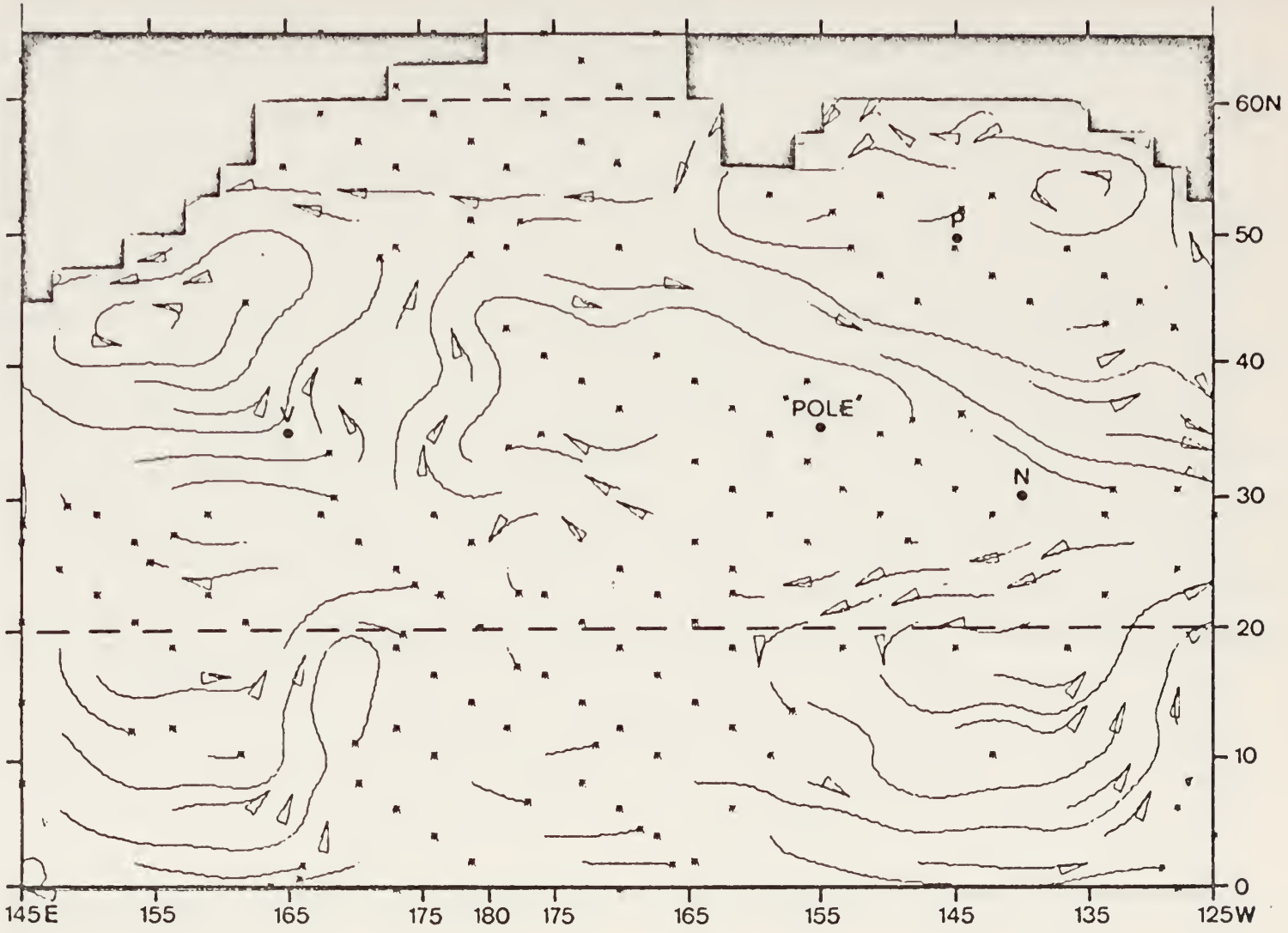

Figure 37. CASE 4: 30-day predicted anomalous currents.

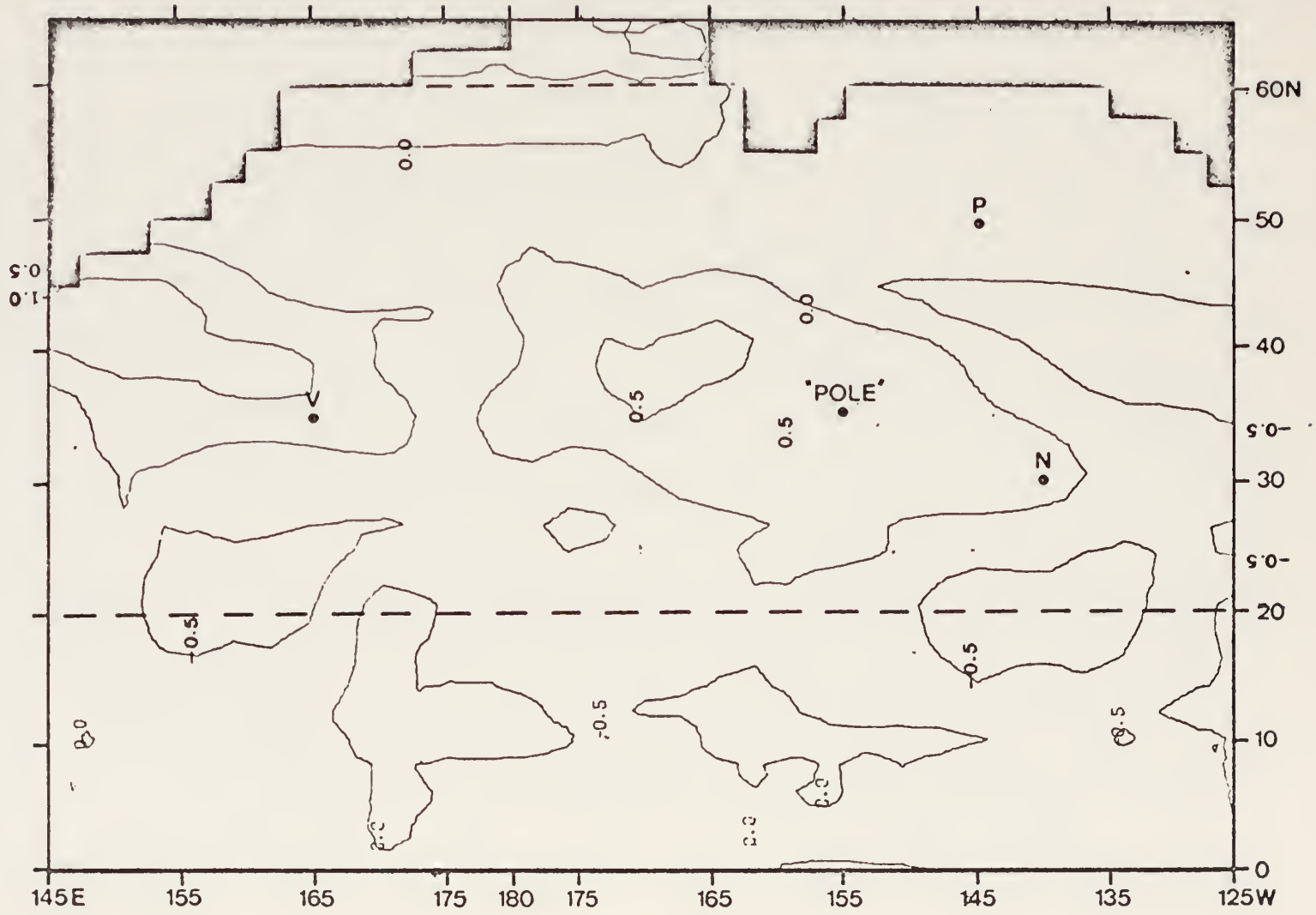

Figure 38. CASE 4: 30-day predicted anomalous temperature field.

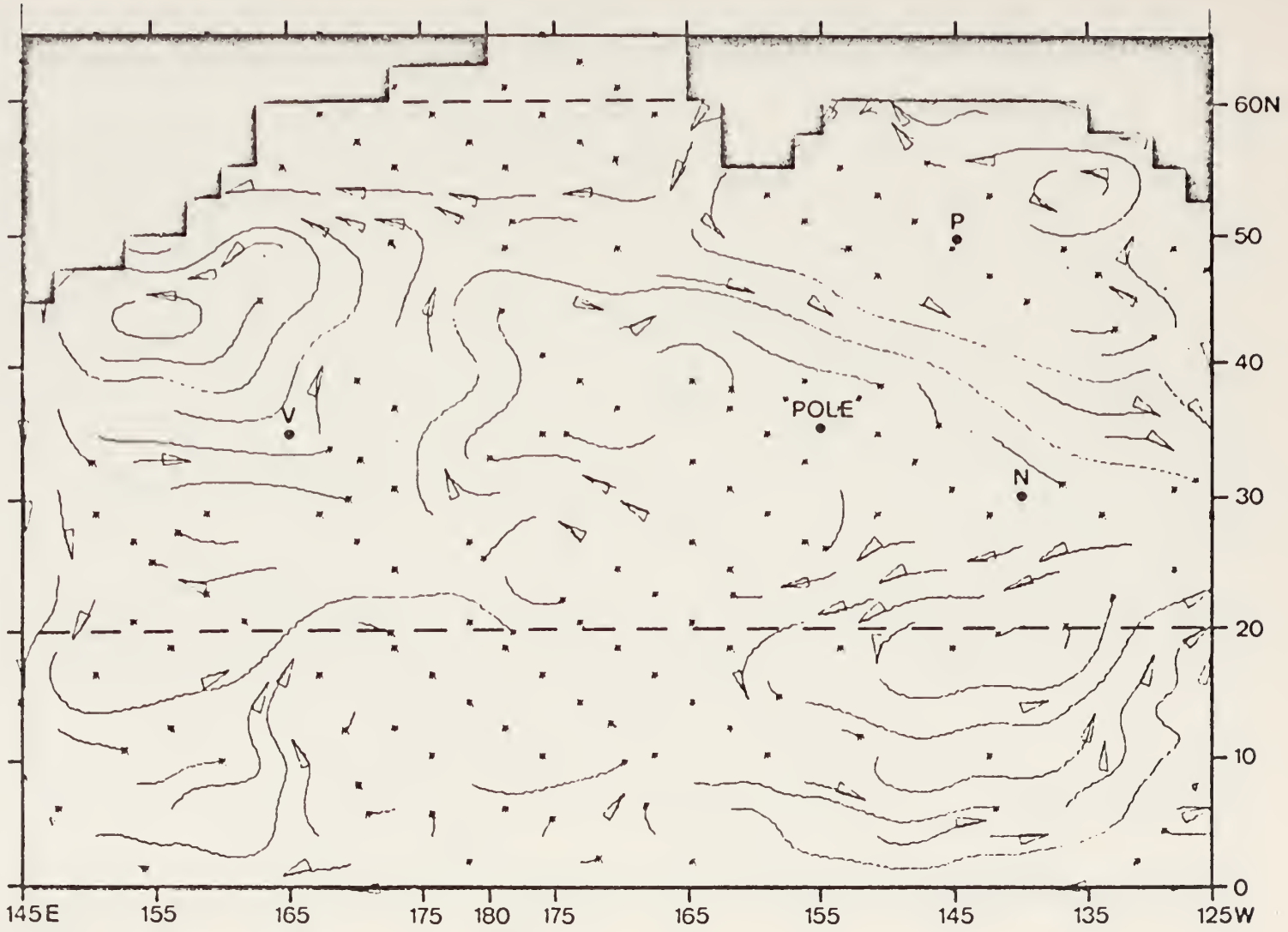

Figure 39. CASE 4: 60-day predicted anomalous currents.

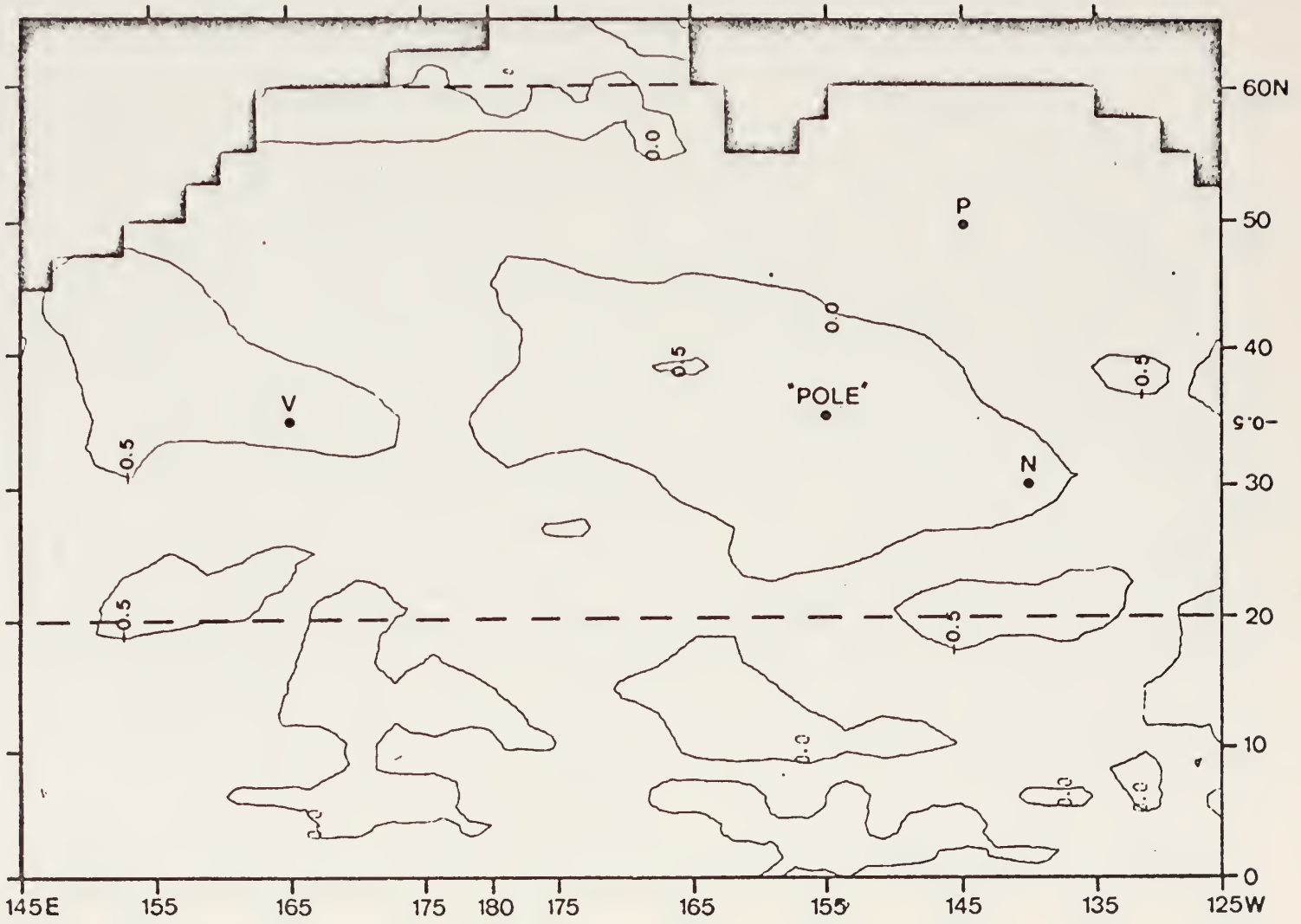

Figure 40. CASE 4: 60-day predicted anomalous temperature field.

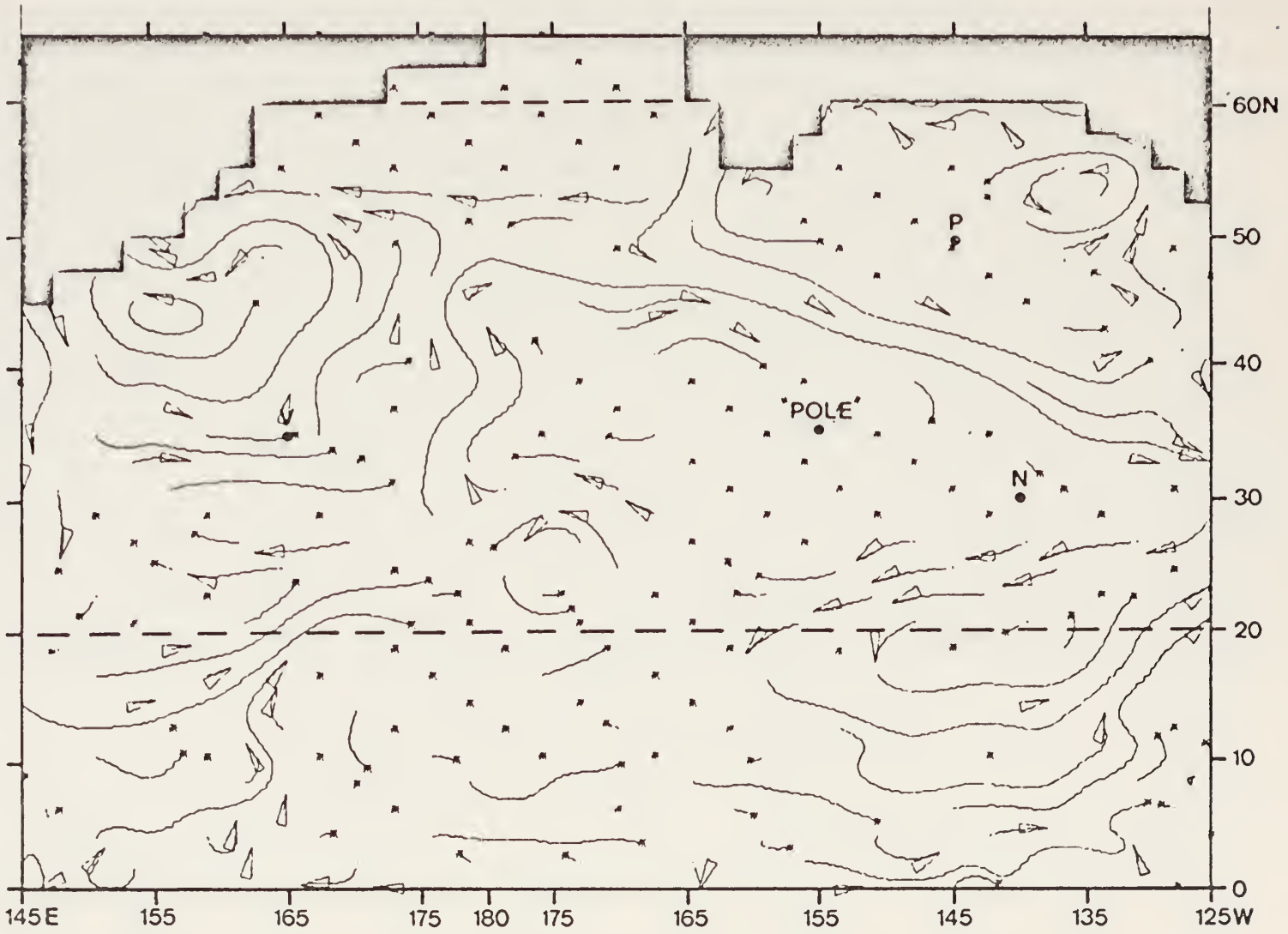

Figure 41. CASE 4: 90-day predicted anomalous currents.

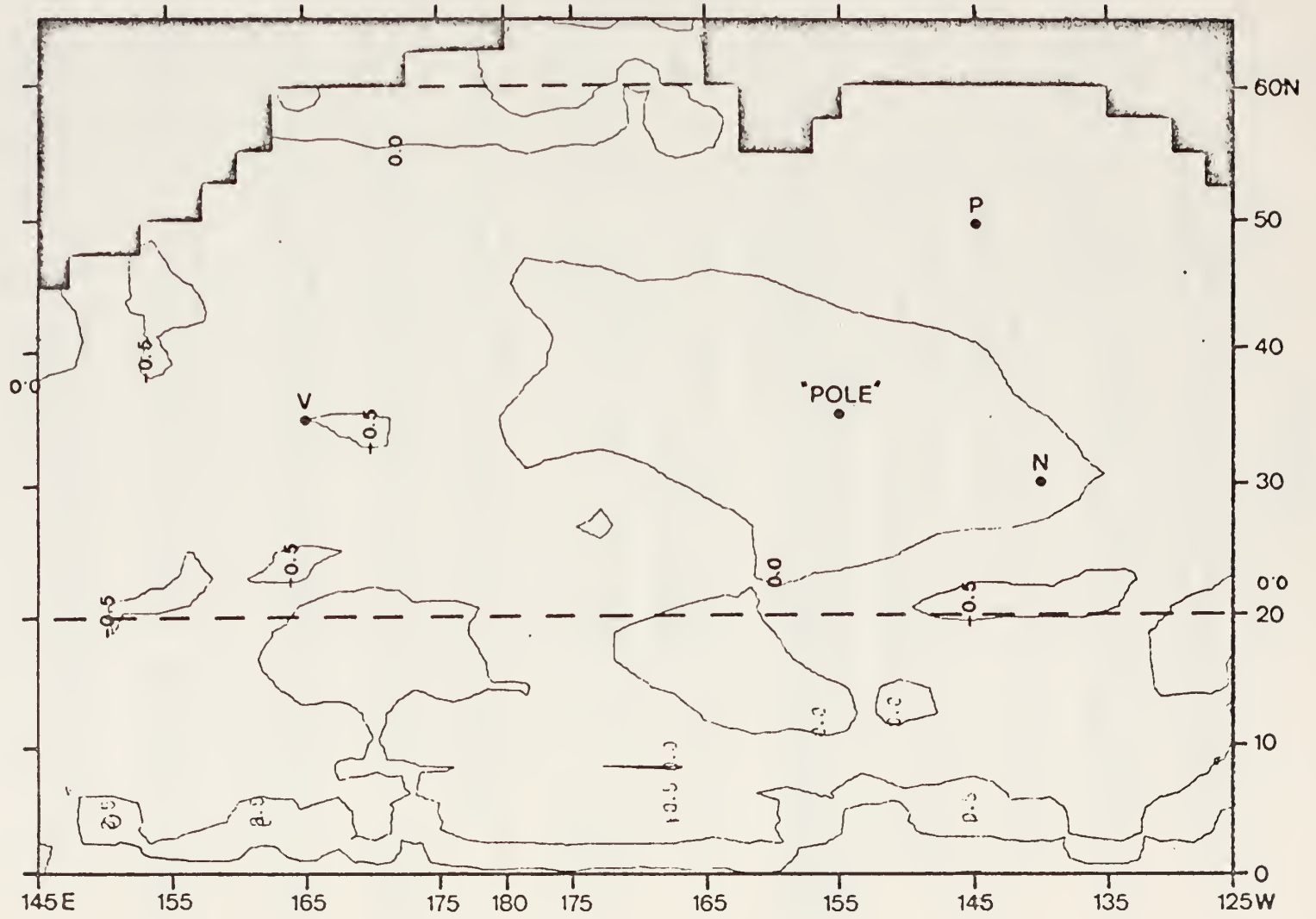

Figure 42. CASE 4: 90-day predicted anomalous temperature field.

REFERENCES

1. Arthur, R. A., 1966: "Estimation of mean monthly anomalies of sea-surface temperature." J. Geophys. Res., 71, 2689-2690.

2. Bjerknes, J., 1966: "A possible response of the atmospheric Hadley circulation to equatorial anomalies of ocean temperatures." Tellus, 18, 820-829.

3. _____, 1969: "Atmospheric teleconnections from the equatorial Pacific." Mon. Wea. Rev., 97, 163-172.

4. _____, 1972: "Large-scale atmospheric response to the 1964-65 Pacific equatorial warming." J. Phys. Oceanogr., 2, 212-217.

5. Davies, R. W., 1975: A numerical parameterization of wind mixing in a time dependent baroclinic oceanic general circulation model. M. S. Thesis, Department of Meteorology, Naval Postgraduate School, Monterey, California, pp. 56.

6. Haney, R. L., 1971: "Surface thermal boundary conditions for ocean circulation models." J. Phys. Oceanogr., 1, 241-248.

7. _____, 1974: "A numerical study of the response of an idealized ocean to large scale surface heat and momentum flux." J. Phys. Oceanogr., 4, 145-147.

8. Jacob, W. J., 1967: "Numerical semiprediction of monthly mean sea surface temperature." J. Geophys. Res., 72, 1681-1689.

9. Namias, J., 1959: "Recent seasonal interactions between north Pacific water and the overlying atmosphere circulation." J. Geo-Phys. Res., 64, 631-646.

10. _____, 1965: "Macroscopic association between mean monthly sea-surface temperature and the overlying winds." J. Geophys. Res., 70, 2307-2318.

11. _____, 1969: "Seasonal interactions between the north Pacific Ocean and the atmosphere during the 1960's." Mon. Wea. Rev., 97, 173-192.

12. _____, 1972a: "Experiments in objectively predicting some atmospheric and oceanic variables for the winter of 1971-72." J. Appl. Meteor., 11, 1164-1174.

13. _____, 1972b: "Large scale and long-term fluctuations in some atmospheric and oceanic variables." In The Changing Chemistry of the Oceans, Nobel Symposium 20, Almquist and Wiksell.

14. Wetherald, R. T., and S. Manabe, 1972: "Response of the joint ocean-atmosphere model to the seasonal variation of the solar radiation." Mon. Wea. Rev., 100, 42-59.

INITIAL DISTRIBUTION LIST

		No. Copies
1.	Defense Documentation Center Cameron Station Alexandria, Virginia 22314	2
2.	Library (Code 0212) Naval Postgraduate School Monterey, California 93940	2
3.	Dr. R. L. Haney, Code 51Hy Department of Meteorology Naval Postgraduate School Monterey, California 93940	3
4.	Lieutenant Kenneth Hunt Fleet Weather Central McAdie Building NAS, Norfolk, Virginia	3
5.	Meteorology Department Code 51 Library Naval Postgraduate School Monterey, California 93940	1
6.	Oceanography Department Code 58 Library Naval Postgraduate School Monterey, California 93940	1
7.	Naval Oceanographic Office Library (Code 3330) Washington, D. C. 20373	1
8.	Commander Naval Weather Service Command Naval Weather Service Headquarters Washington Navy Yard Washington, D. C. 20390	1
9.	Fleet Numerical Weather Central Naval Postgraduate School Monterey, California 93940	1
10.	Environmental Prediction Research Facility Naval Postgraduate School Monterey, California 93940	1

11. Dr. W. L. Gates — 1
Physical Sciences Department
Rand Corporation
1700 Main Street
Santa Monica, California 90406

12. Dr. J. Huang — 1
Great Lakes Environmental Research Lab - NOAA
2300 Washtenaw Avenue
Ann Arbor, Michigan 48104

13. Dr. J. Namias — 1
Department of Oceanography
Scripps Institution of Oceanography
La Jolla, California 92037

14. Lt. R. W. Davies — 1
Tactical Electronic Warfare Squadron 129
NAS, Whidbey Island
Oak Harbor, Washington 98277

15. Lt. D. Hinsman — 1
Fleet Numerical Weather Central
Naval Postgraduate School
Monterey, California 93940

16. Dr. R. L. Elsberry, Code 51Es — 1
Department of Meteorology
Naval Postgraduate School
Monterey, California 93940

17. Dr. R. T. Williams, Code 51Wu — 1
Department of Meteorology
Naval Postgraduate School
Monterey, California 93940

18. Dr. G. J. Haltiner, Code 51Ha — 1
Department of Meteorology
Naval Postgraduate School
Monterey, California 93940

19. Dr. R. C. Alexander — 1
Physical Sciences Department
Rand Corporation
1700 Main Street
Santa Monica, California 90406

Thesis
H947 Hunt
c.1 The prediction of sea-surface temperature anomalies using a 10-level primitive equation model.